Discover Chemical Engineering

Discover

Review

Combining experimental and theoretical insights for reduction of CO_2 to multi-carbon compounds

Ian Brewis[1] · Rana-Faisal Shahzad[1] · Robert W. Field[1] · Abdesslem Jedidi[2] · Shahid Rasul[1]

Received: 24 December 2021 / Accepted: 8 February 2022
Published online: 04 March 2022

Abstract
The electrochemical reduction of carbon dioxide is a promising method for both recycling of atmospheric CO_2 and storing renewably produced electrical energy in stable chemical bonds. In this paper, we review the current challenges within this promising area of research. Here we provide an overview of key findings from the perspective of improving the selectivity of reduction products, to serve as a contextual foundation from which a firmer understanding of the field can be built. Additionally, we discuss recent innovations in the development of catalytic materials selective toward C_3 and liquid products. Through this, we form a basis from which key mechanisms into C_3 products may be further examined. Carbon–carbon (C–C) bond formation provides a key step in the reduction of CO_2 to energy dense and high value fuels. Here we demonstrate how variations in catalytic surface morphology and reaction kinetics influence the formation of multi-carbon products through their impact on the formation of C–C bonds. Finally, we discuss recent developments in the techniques used to characterise and model novel electrocatalysts. Through these insights, we hope to provide the reader with a perspective of both the rapid progress of the field of electrocatalysis, as well as offering a concise overview of the challenges faced by researchers within this rapidly developing field of research.

Keywords Electrochemistry · Catalysis · CO_2 reduction · Energy storage

1 Introduction

Fossil fuels form the cornerstone of industrial and economic growth globally, accounting for over 87% of the world's total energy consumption [1, 2]. Dwindling fuel reserves and mounting environmental damage as a result of burning fossil fuels demonstrate the need to move beyond our global dependence on non-renewable sources of energy. As of 2015, the remaining oil and natural gas reserves were estimated at 1697.6 billion barrels and 186.9 trillion cubic meters respectively. Based on global consumption levels as of 2015 and the remaining supply of fossil fuels at that time, it was estimated that around 50 years of oil and gas remain [2].

The burning of such large quantities of fossil fuels, particularly in the transport sector, has resulted in the uncontrolled release of CO_2 into the atmosphere, significantly contributing toward climate change [3–5]. This realisation has led to considerable efforts being made to transition from fossil fuels toward low carbon and renewable alternatives such as biofuels, hydroelectric power, solar, wind, geothermal, and nuclear energy [1]. Whilst some low carbon

✉ Abdesslem Jedidi, ajedidi@kau.edu.sa; ✉ Shahid Rasul, Shahid.Rasul@Northumbria.ac.uk; Ian Brewis, Ian3.Brewis@Northumbria.ac.uk; Rana-Faisal Shahzad, Rana-Faisal.Shahzad@Northumbria.ac.uk; Robert W. Field, Robert.Field@Northumbria.ac.uk | [1]Faculty of Engineering and Environment, Northumbria University, Ellison Pl, Newcastle Upon Tyne NE1 8ST, UK. [2]Department of Chemistry, King AbdulAziz University, Abdullah Sulayman, Jeddah 21589, Saudi Arabia.

energy sources such as nuclear and hydroelectric energy are being implemented on a large scale [1], most alternatives to fossil fuels, such as solar and wind, have been unable to achieve this due to intermittent operating times and are incapable of consistently meeting global energy demands in their current state [6]. A key method in tackling this inherent intermittancy is through the conversion of otherwise surplus energy into a medium which is both portable and storable so that it may be implemented wherever and whenever it is needed, much like fossil fuels are used today [3, 7–11]. CO_2 reduction poses an attractive method of converting said energy. By using the abundant greenhouse gas CO_2 to produce carbonaceous fuels compatible with existing infrastructure it effectively forms a carbon neutral cycle for the production of hydrocarbons [12–14]. An example of such a cycle as this can be observed in Fig. 1.

By implementing carbon capture technology to siphon waste CO_2 from the atmosphere, as well as natural and industrial processes. CO_2 reduction aims to mimic the natural process of photosynthesis (i.e. "artificial photosynthesis") [3, 6], effectively managing atmospheric levels of CO_2 whilst providing a carbon neutral source of fuels. An added bonus of recycling CO_2 via electrochemical reduction is that the fuels produced are highly compatible with existing technology which would otherwise be powered by fossil fuels, with most only requiring minor modifications [7, 15, 16].

It is for these reasons that the electrochemical reduction of CO_2 has begun to see notable interest within the field of electrochemistry [15, 17–20]. The electrochemical reduction of CO_2 however is still an emerging technology. There are significant challenges to current electrocatalyst performance, including: issues regarding energy efficiency, reaction selectivity both between CO_2 reduction (CO_2RR) products and with the competing hydrogen evolution reaction (HER), as well as overall conversion rate. Before carbonaceous fuels produced via the reduction of CO_2 can be considered as a viable method of energy storage, each of these challenges must first be addressed [20].

A 2008 review by Hori [21] examined many elemental metal catalysts in terms of their overall catalytic performance and product selectivity. Since then, considerable work has been conducted into improving the activity and selectivity of reduction products. A overview of some of the most active electrocatalysts selective towards specific products can be observed in Table 1. Despite the stability of the CO_2 molecule [22], it can be reduced to simple products requiring only a 2-electron transfer process such as CO and HCOOH with low overpotential and high Faradaic efficiency. For larger products requiring higher numbers of electron transfers however, such as ethylene or alcohols, markedly higher overpotentials and lower selectivities among CO_2RR products are observed [20].

The aim of this review is to examine and discuss some of the history of electrochemical CO_2 reduction, as well as its more recent advances, to provide the reader with an overview of the field itself. Through this, this review aims to provide a sense of where the field has come from, as well as how it maybe further develop in the future [17, 18, 17–18]. Among the topics discussed within this paper are: the CO_2 reaction processes; including initial activation, catalyst design; both past and present, and finally the use of computational methods to improve our fundamental understanding of the CO_2 reduction reaction (CO_2RR).

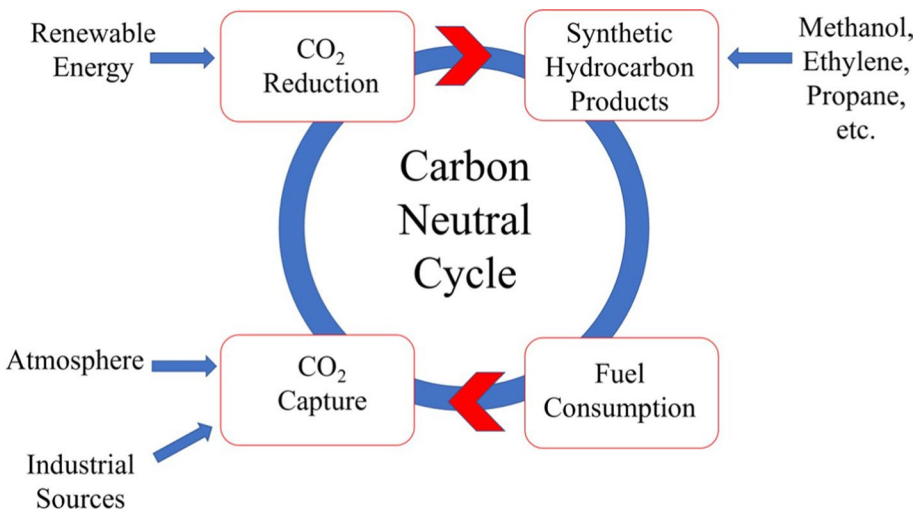

Fig. 1 The "carbon neutral cycle". Here atmospheric CO_2 is captured and reduced to form synthetic hydrocarbons in the order of C_1 to C_3 chains (adapted from [3])

Table 1 Highly active electrocatalysts selective toward specific CO_2RR products [20]

CO_2RR product	Electrocatalyst	Faradaic efficiency (%)	Overpotential (V)	j_{total} (mA cm^{-2}	Electrolyte (CO_2 saturated)	Ref.
HCOOH	Pb	97.4	− 1.19 V	5.0	0.1 M $KHCO_3$	[25]
	Sn	88.4	− 1.04 V	5.0	0.1 M $KHCO_3$	[25]
	Pd nanoparticles/C	99	− 0.15 V	2.4–7.0	2.8 M $KHCO_3$	[26]
	$Pd_{70}Pt_{30}$ nanoparticles/C	90	− 0.36 V	4.0–7.5	0.2M PO_4^{3-}buffer	[27]
CO	Au	87.1	− 0.64 V	5	0.1 M $KHCO_3$	[25]
	Au nanoparticles	97	− 0.58 V	3.49 ± 0.61	0.1 M $KHCO_3$	[28]
	OD-Au nanoparticles	> 96	− 0.25 V	2–4	0.5 M N_aHCO_3	[29]
	Ag	94	− 0.99 V	~ 5	0.1 M $KHCO_3$	[30]
CH_4	Cu poly	40.4	− 1.34 V	~ 7	0.1 M $KHCO_3$	[31]
	Cu(210)	64	− 1.29 V	5	0.1 M $KHCO_3$	[32]
C_2H_4	Cu poly	26	− 1.13 V	1–2	0.1 M $KHCO_3$	[31]
	O_2 plasma-treated Cu	60	− 0.98 V	~ 15	0.1 M $KHCO_3$	[33]
	Cu-halide	60.5–79.5	− 2.11 V	46.1–39.2	3 M KBr	[34]
	Graphite/carbon NPs/Cu/PTEE	70	− 0.63 V	75–100	7 M KOH	[35]
CH_3OH	Pt_xZn nano-alloys/C	81.4	− 0.90 V	~ 3	0.1 M $NaHCO_3$	[36]
	Co nanoparticles	71.4	− 0.90 V	4	0.1 M $NaHCO_3$	[37]
C_2H_5OH	Cu poly	9.8	− 1.14 V	~ 0.6	0.1M $KHCO_3$	[31]
	Cu_2O	9-16	− 1.08 V	30–35	0.1 M $KHCO_3$	[38]
	CuO nanoparticles	36.1	N/A	~ 11.7	0.2 M KI	[39]
	Cu/CNS	63	− 1.29 V	2	0.1 M $KHCO_3$	[40]

2 CO_2 reaction conditions

2.1 Methods of CO_2 reduction

Broadly speaking, the various methods of CO_2 reduction can be classified in the following four categories: thermochemical, biochemical, photochemical and electrochemical reduction. Thermochemical CO_2 reduction methods have been in use for a number of years, an example of which is the formation of methanol using CO_2 and H_2 chemical feed-stocks under a catalyst typically composed of $Cu/ZnO/AlO_3$. This process, similar to the current industrial method for the formation of methanol from syngas [3, 41–44], requires high temperatures and pressures of around 220 to 330 °C and 50 to 100 atm respectively [43, 44]. Similarly, at lower pressures, CO_2 and H_2 can be used as reactants to form hydrocarbons using Fischer–Tropsch style catalysts, albeit at still elevated temperatures [45, 46]. Consequently, due to the high temperatures and pressures required, thermochemical reduction methods are highly energy intensive, and are therefore most commonly driven by fossil fuels. Biochemical methods commonly employ the use of enzymes or autotrophic organisms in order to capture and convert CO_2 into complex products [47, 48]. Photochemical methods, by contrast, use photo- and electrocatalysts in order to mimic natural photosynthesis by both splitting water and reducing CO_2 using sunlight to drive the reaction process [49–51]. By convention, research in both biochemical and photochemical reduction methods aim to use sunlight as a near unlimited source of energy to convert CO_2 to energy dense fuels under ambient conditions. A limitation of this however is that such methods neglect the use of other renewable energy sources.

Electrochemical reduction methods, unlike biochemical and photochemical methods, are not limited to a single renewable energy source, and with the use of a well suited electrocatalyst, are capable of effectively reducing CO_2 under ambient conditions [15, 52]. Due to this, electrochemical methods can be easily adapted to be used in conjunction with almost any renewable energy source, particularly as most renewables are used to generate electrical energy. Additionally, high energy efficiencies observed at mild reaction conditions make electrochemical reduction methods an attractive avenue for the reduction of CO_2 to fuels [53, 54]. Yao et al. for example, reduced CO_2 to hydrocarbons with an overall selectivity of 47.8% across all carbonaceous products, predominantly in the range of C_8 to C_{11} [55]. Such results were produced based on a novel Fe–Mn–K tri-metallic electrocatalyst, producing mainly fuels in a range compatible with most modern aircraft. Another such example is that of Sumit et al. who reduced CO_2 to CO in an alkaline flow electrolyzer with

an energy efficiency of 64% using an Au electrode [56]. Such values of efficiency rival that of the hydrogen evolution reaction (HER) using a Pt catalyst in alkaline electrolyte [57].

2.2 The activation of CO_2

Formed through the combustion of organic matter, CO_2 is a particularly stable molecule [22, 58]. Due to this, it is kinetically challenging to convert CO_2 to products due to the high activation energy required for the reduction process [12, 59]. The single electron reduction of CO_2 to CO_2^- has been shown to have a high thermodynamic potential of $E^o = -1.90V$ versus the standard hydrogen electrode (SHE) in aqueous media $(pH = 7)$ [29, 60–62]. This initial activation step is critical as it forms the rate limiting step of the CO_2RR [18]. The coordination of this intermediate additionally determines the whether the CO_2 molecule will be reduced to CO or formate following the transfer of 2 electrons [63]. For example, post-transition metals selective toward the formation of formic acid, such as Pb [64], Sn [65], Bi [66, 67] and In [68] prefer to bind CO_2 via oxygen. Transition metals such as Cu [69] and Ag [70] however prefer to bind via carbon, resulting in the production of CO. Bagger et al. [71] however, suggests an alternative. For Cu surfaces they demonstrate how oxygen bonded HCOO* is stabilised more effectively than carbon bonded COOH*, suggesting a possible oxygen-bound pathway. In addition to this, they suggest the formation of formic acid to be related to the relative standing of the binding energies of H and COOH*. This was supported by the lack of experimental evidence showing a lack of HCOO* surface saturation prior to the onset of HER, despite adsorption energy values suggesting an earlier onset of HCOO* production [72–75].

Selectivity of the reaction pathway towards products such as this can be further improved using the appropriate catalyst [25, 27]. It should be noted however, that the choice of material alone does not solely dictate product selectivity. One clear example of this was shown in a recent work by Scholten et al. [76] which demonstrated how highly ordered single-crystal Cu surfaces produced mainly hydrogen. By contrast, it was found that only through the introduction of surface defects such as with etching and plasma pre-treatment methods that significant amounts of hydrocarbons were produced. When considering the activation of CO_2, the following 4 equations govern the reactions taking place

$$* + CO_2 + H^+ + e^- \rightarrow {}^*COOH \tag{1}$$

$$* + CO_2 + H^+ + e^- \rightarrow {}^*OCHO \tag{2}$$

$$* + CO_2 + e^- \rightarrow {}^*CO_2^- \tag{3}$$

$$* + H^+ + 2e^- \rightarrow {}^*H^- \tag{4}$$

where * denotes a binding site on the catalyst surface. Here *COOH is considered to likely be the be intermediate for CO formation and *OCHO the likely intermediate in the formation of formic acid for transition and post-transition metals [77].

A 2017 work by Adrien et al. [78], postulates that the reaction takes place in agreement with previous literature, however with subtle changes. Rather than following only the concerted proton–electron transfer (CPET) reactions as shown in Eqs. (1) and (2), the CO_2RR could instead follow a combination of both a CPET reaction and sequential proton–electron transfer (SPET). For the SPET reaction, the single reaction step depicted in Eq. (1) instead takes place as a 2-step process consisting of the initial activation of CO_2 as shown in Eq. (3), followed by

$${}^*CO_2^- + H^+ \rightarrow {}^*COOH. \tag{5}$$

It was suggested in the same work by Adrien et al. that the conditions affecting the ratio of CPET to SPET reactions were tied to the local pH in the vicinity of the catalyst surface. In the vicinity of pH 3 for example, it was found that the SPET pathway became competitive with CPET, in agreement with experimental results, which saw a dramatic increase in the faradaic efficiency toward CO production. This pH dependence of CO_2 reduction pathways, and possibly differing pH dependence compared to the competing hydrogen evolution reaction (HER) was used to explain the strong pH dependence of product selectivity for graphite-immobilized CO-protoporphyrin, where H_2 was observed as the main reduction product at pH 1, and CO as the main product at pH 3 [79, 80]. This pH dependence of reaction products is further agreed upon by Koper [81], who suggested that due to the nature of this pH dependence, an optimal pH for desired reaction products must be attainable, with a suitable catalyst. The pH dependent, decoupled proton–electron reaction pathways however, Koper explained, are more prevalent if the interaction between the catalyst and intermediates is weak, as CPET

reactions dominate where catalyst-intermediate interactions are strong, resulting in a low pH dependence of reaction products. Not only have reaction conditions been shown to be sensitive toward electrolyte pH, but also to the nature of the electrolyte used. Monteiro et al. [82] for example, demonstrated how a lack of metal ions prevents the formation of CO on Cu surfaces. Their work highlighted the crucial importance of short-range electrostatic interactions between the electrolyte and catalytic surface in promoting CO_2RR.

For the formation of formate and formic acid, a similar situation is observed, particularly for molecular catalysts such as Rh, In and Sn metalloprotoporphyrins which were reported to produce formic acid selectively in aqueous electrolyte [83]. It should be noted however that the formation of formate using an Rh protoporphyrin is only capable at elevated pressures [84], with Rh ordinarily producing H_2 as the main product under ambient conditions [85]. Density functional theory (DFT) studies into molecular catalysts such as those mentioned previously showed a strong pH dependence on the formation of formic acid [86]. Here it was found that within a strongly acidic electrolyte the HER is favourable, following the same reaction path as outlined in Eq. (4). This result was in strong agreement with the literature [87, 88]. From the production of an anionic hydride as shown in Eq. (4), the anion binds to the carbon atom of CO_2 like so

$$CO_2 + H^- \rightarrow HCOO^-. \tag{6}$$

The subsequent stability of the $HCOO^-$ intermediate can then dictate the formation of either CO or HCOOH. Discussion of this hydride dependent reaction pathway has been further examined for a range of catalysts observed to produce formic acid among their reaction products. Such catalysts include copper-hydride nanostructures [89], palladium electrodes [26], and in solution [90].

When considering Eqs. (3) and (4), as opposed to Eqs. (1) and (2), the pH sensitivities resulting from the charge of key intermediates suggests the another challenge when designing and implementing an electrochemical cell. For CO_2 reduction, this challenge is ensuring an optimal local and system-wide pH for the production of desired products. This is true in particular for reduction products formed following a 2-electron transfer such as CO and HCOOH. The formation of larger and more energy dense products from the CO_2RR is however another desired result within the field of electrochemistry. As such, the following section shall cover some works published in this regard.

2.3 Formation of multi-carbon compounds

In order to form larger and more energy rich products such as hydrocarbons and alcohols, CO_2 reaction intermediates must undergo additional reaction steps requiring the transfer of multiple electrons. Due to the added complexity of the reaction, a clear drop in selectivity can be observed for C_2 and greater products when compared with the production of simpler products such as CO and formate which require fewer reaction steps. As well as this, notably higher overpotentials can also be observed [17]. Figure 2 illustrates some of the proposed reaction pathways to larger and more complex products following the formation of CO.

It should be noted that following the initial activation of the CO_2 molecule, the standard reduction potentials for sequential reaction steps under ambient conditions are relatively low. Even for the formation of large molecules such as ethanol and propanol, reduction potentials are of the order of $\approx -0.5V$ [93, 94]. Whilst this would suggest the formation of hydrocarbons and alcohols would not be much more energetically demanding than the formation of formate or CO, the formation of larger hydrocarbons have been shown to be kinetically challenging [94, 95]. This is due to the reaction kinetics involved in transferring large numbers of electrons, as well as the large structures of multiple carbon products involved in the reaction.

The formation of C_{2+} and greater products such as propane and butane from the CO_2RR is of particular interest due to the greater energy density provided by these products. Copper, and copper-based catalysts have been shown as being almost exclusively capable of providing the necessary conditions to form Carbon–carbon bonds at significant current densities [21, 69]. Copper demonstrates an intermediate adsorption energy for CO, providing more ideal conditions for the formation of C–C bonds. Metals with higher binding energies, such as Pt, Ni, Fe and Ti, for example, show a greater selectivity toward hydrogen due to tighter CO binding on the catalyst surface [21, 96, 97]. By contrast, metals such as Au, Ag and Zn, which exhibit a lower adsorption energy, produce mainly CO as the intermediate desorbs from the catalyst surface before further reactions can take place [25, 98–100]. A more complete picture of the binding energies for Cu with various reaction intermediates can be observed in Fig. 3.

A small number of other catalyst designs have been proposed including NiGa, PdAu, NiP and N-doped carbon catalysts which have been capable of producing C_2 and greater products, however none have been able to do this as efficiently

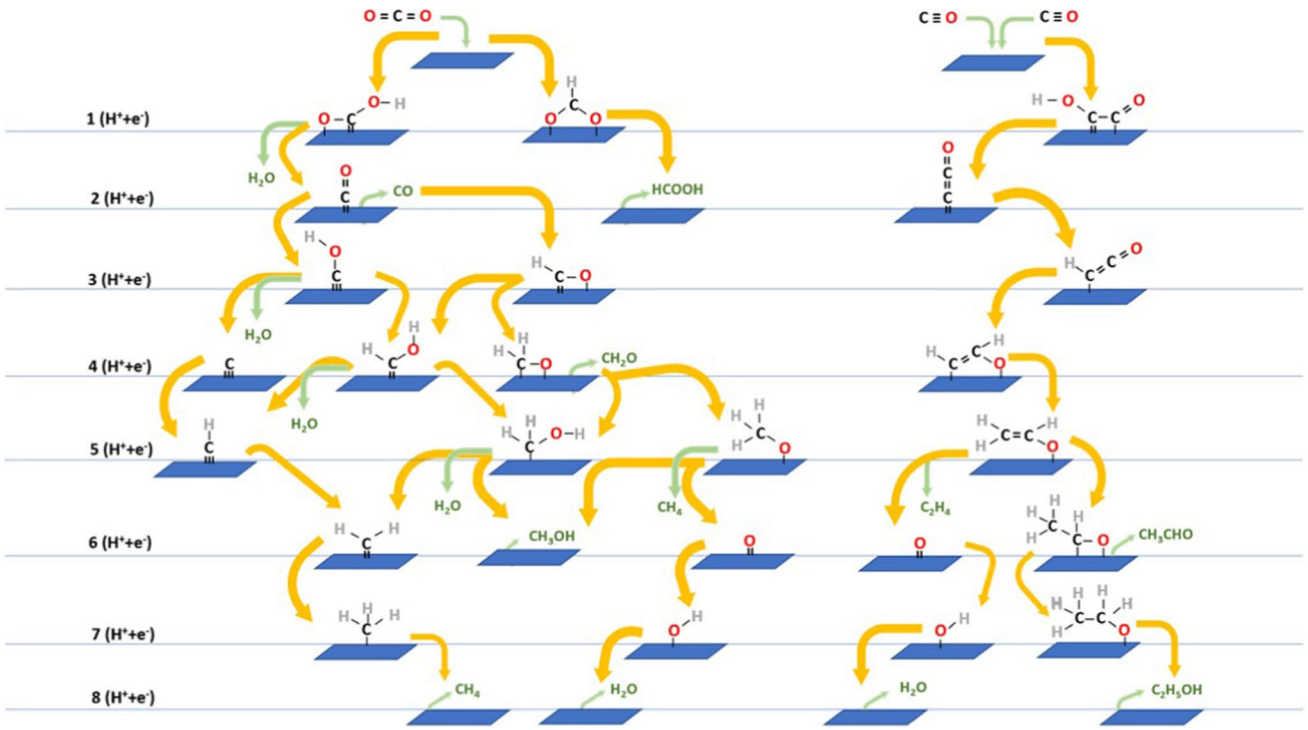

Fig. 2 Molecular reaction pathway diagram of the electrochemical reduction of CO_2 to larger products (adapted from [91, 92])

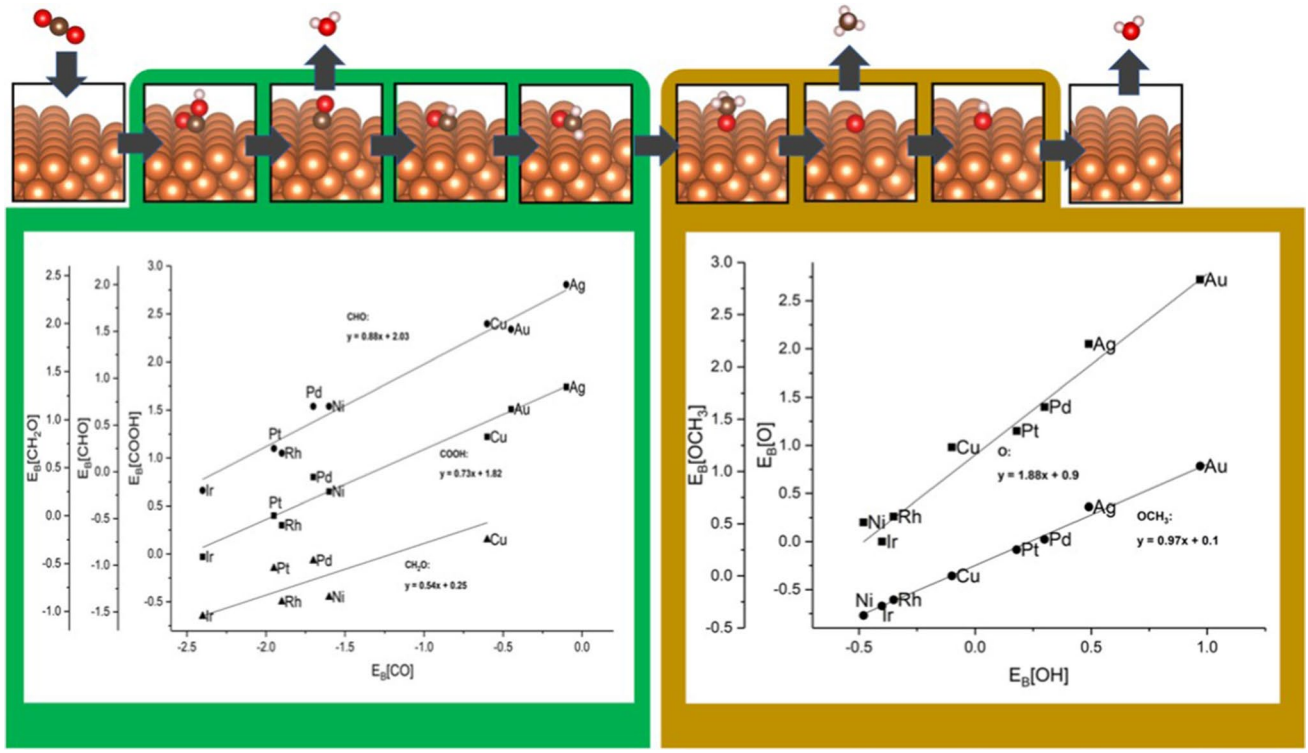

Fig. 3 Adsorption energy scaling. A proposed pathway for the reduction of CO_2 to CH_4 for a metal surface is shown at the top of the image and the adsorption energies of bound intermediates on the fcc (face-centred cubic)(211) facet are shown on the two lower figures. (More tightly bound adsorbates correspond to more negative binding energies.) The adsorption energies of adsorbates bound to the surface by carbon (pictured left) and by oxygen (pictured right) are correlated and plotted against the binding energy of key intermediates CO and OH respectively (adapted from [101])

as copper as of yet [102–105]. Recently, notable developments in improving the selectivity of copper catalysts toward C_2 products have been observed in a number of ways. Examples of this include altering the catalyst surface structure, such as through high-surface-area oxide-derived (OD) copper, as well as by altering the electrolyte composition and by employing organic films on copper [35, 106–108].

Another point of interest in the formation of C_2 and greater products is the possibility of liquid products. Liquid fuels provide both a higher energy density and greater economic value, as well as a simpler method of storage [109]. Due to this, the study of the reaction pathway from CO_2 to the most typically produced liquid fuels from the CO_2RR such as ethylene and ethanol have been subject to a plethora of theoretical [110–114] and experimental studies [32, 52, 115–118].

From prior experimental studies, two pathways for ethylene production have been observed. The first takes place mainly on Cu(111) at high overpotential using a shared intermediate with methane, and the second on Cu(100) at lower overpotential which does not yield methane as a product [117]. The second method also differs from the first in that it is pH independent. It forms Carbon–carbon bonds through the formation of a CO dimer from adsorbed surface materials, as opposed to individual transfers of protons and electrons [69, 84, 91, 119]. As a consequence of this, the production of ethylene is favoured on the face-centred cubic (fcc) (100) facet as local pH can be optimised toward CO formation over the HER with no impact on the selectivity of C_2 products. The formation of ethylene using the fcc(100) facet is in stark contrast with the formation of methane from copper electrodes which has been observed to be most actively produced on the fcc(211) facet [25, 120]. Numerous experimental [52, 115] and theoretical works [110–112] however confirm the different reaction pathways taken when producing either ethylene or methane. Such works demonstrate drastic differences in the reaction conditions required to form larger hydrocarbons over smaller products. Based on results from DFT calculations, it is believed that at more negative potentials the dimerisation of CO is replaced by a more favourable reaction based on the coupling of *CO and *CHO. The reaction between these intermediates is believed to be due to the lower activation energy of the latter reaction [112, 121]. DFT calculations additionally confirm the tendency for CO dimerisation to be favoured on Cu(100) facets. Furthermore, DFT calculations provide additional insights into C–C bond formation in this case, such that the CO dimer is energetically favoured in the presence of a water layer, a local electric field and in the presence of alkali cations [111, 113]. This pH sensitivity has been attributed to the rate-determining step in the formation of C–C bonds involving a decoupled proton–electron transfer. This hypothesis is based on a combination of both DFT calculations and experimental data [110].

A recent report by Perez-Gallent et al. [122] observed the formation of a hydrogenated CO-dimer (OCCOH) intermediate during CO reduction using Fourier transform infrared spectroscopy at low overpotentials in LiOH solutions. All results for this work were supported with DFT calculations. In agreement with previous literature, the formation of CO dimers was structurally sensitive; only being observed on the fcc(100) facet. Thus it was concluded, in agreement with prior works, that the formation of the dimer was favoured both thermodynamically and kinetically on Cu(100) compared to Cu(111) [111, 117].

Whilst the effect of adding certain organic layers to copper catalysts such as pyridium [106] or triazole [107] is yet to be fully understood, studies have suggested the modification of copper with such layers results in an enhanced selectivity toward the production of C_2 products. Currently however, this effect is believed to possibly be due to local pH effects caused by the presence of such organic materials. One recent study by Hoang et al. [107] for example, reported faradaic efficiencies for the production of C_2H_4 and C_2H_5OH reaching approximately 60 and 25% respectively for a cathode potential of − 0.7 V vs. RHE. The same study also reported a total current density of $\sim -300\,\mathrm{mA/cm^2}$, one of the highest catalytic activities at low potential reported to date.

Despite the volume of research published into possible reaction pathways towards the formation of C–C bonds however, current faradaic efficiencies for the formation of C_3 products such as propane and propanol remain relatively low [64, 123]. Previous studies have suggested that by promoting a high selectivity toward the formation of C_2, the right conditions to produce C_3 or larger products could be achieved. The current understanding of the reaction mechanisms towards the formation of propane and larger hydrocarbons however, is still unclear. Due to the large number of electron transfers involved, developing a clear picture of a reaction pathway would be a time-consuming and difficult process. An alternative method of examining C_3 however, as shown by Bagger et al. [124] could use descriptors for product distribution on specific facets to categorise reaction products by comparing coordination number distribution and the binding energies of intermediates. Currently however, researchers propose either the further use of CO as a reaction intermediate, or the formation of C–C bonds between C_1 and C_2 intermediates [31, 125, 126]. Current research also seems to suggest a likely intermediate toward C_3 being formed through the coupling of CO and C_2H_4 precursors [127, 128]. A 2019 study by Wang et al. [123] reported the highest Faradaic efficiency to date for the formation of propanol of $33 \pm 1\%$ with a cathodic energy conversion efficiency of 21% for metal-doped copper catalysts. Due to the increased energy density and

ease of storage of liquid fuels, a greater understanding of the reaction mechanisms required to form C–C bonds in order to produce larger hydrocarbon and alcohol products could prove revolutionary in improving the commercial viability of the electrochemical reduction of CO_2.

3 Optimising catalyst structure for the formation of fuels

Following Hori's review in 2008 [84], the development of catalysts has seen drastic improvement. From his results it was found, as previously stated, that copper most effectively produces fuels from the electrochemical reduction of CO_2 (see Table 2).

Among the metals tested, it was found consistently that the formation of CO from the CO_2RR occurred on face centred cubic (fcc) transition metal lattices [84, 129, 130], suggesting a strong dependence on the surface morphology on overall product selectivity. Due to this, considerable work has been conducted aimed toward optimising catalyst surface structure to produce an electrocatalyst highly selective toward a given CO_2RR product, whilst minimising the effect of the competing HER. Studies have included the alloying of surface materials [24, 131–134], production of nanoparticles [12, 65, 135] as well as an Ag "nano-coral" structure prepared by an oxide-reduction method in the presence of chloride anions in an aqueous medium [136].

3.1 Bimetallic alloy catalysts

With regards to alloy catalysts, the introduction of heteroatoms to form bimetallic alloys allows for both the structural and electronic properties of the catalyst to be altered due to the interaction between the two elements involved. For example, one study using Ru–Pd catalysts saw in increase in the selectivity of formic acid production from 70% at $-0.7\mathrm{V}$ for pure Pd catalysts to 90% at $-1.1\mathrm{V}$ vs. NHE [137]. Similarly, a 2015 work by Rasul et al. [132] saw a dramatic improvement in the selectivity of CO production through the introduction of In hetero-atoms into an oxide-derived copper catalyst structure. Here a total Faradaic efficiency of 95% at $-0.7\mathrm{V}$ vs. RHE was observed, higher than values observed for either Cu or In separately. It was suggested in this study that the enhanced Faradaic efficiency toward the production of CO was due to the suppression of the HER through structure changes. These changes were believed to have been caused by the preferential binding sites of In within the Cu lattice, based on the high overpotentials observed for HER for In in comparison with copper. Figure 4 demonstrates the preferential binding sites of In within the Cu lattice based on calculations in a follow-up paper by Jedidi et al. [131] demonstrating the preference for In atoms to replace Cu atoms in positions of low coordination such as defects and the fcc(211) facet step-site.

3.2 Nanoparticles

An alternative approach to optimising catalyst selectivity through morphological changes is the fabrication of nanostructures such as nanoparticle and nano-coral structures. The size of metal nanoparticles has been reported to have a strong influence on both the activity and selectivity of CO_2 reduction catalysts [138–140]. For example, a 2014 study by Reske et al. [140] on Cu nanoparticles 2–15 nm in diameter found that for nanoparticles below 5nm the formation of hydrocarbons such as methane and ethylene were suppressed, resulting in an enhanced selectivity toward CO and H_2 formation. Such changes in selectivity were attributed to higher concentrations of low-coordinated surface sites, resulting in stronger chemisorption, as well as boosted catalytic activity. A similar study on the size dependency of Au

Table 2 Faradaic yields in CO_2 reduction on fcc metal electrodes for experiments at 5 mA cm^{-2} current density in a 0.1 M $\mathrm{KHCO_3}$ buffer at $18.5°\mathrm{C}$. Adapted from Peterson et al. [101]

Electrode	V vs. RHE	Hydrocarbons/organics	CO	HCOOH	H_2	Total
Ni	−1.09	2.1	0.0	1.4	88.9	92.4
Cu	−1.05	72.3	1.3	9.4	20.5	103.5
Pd	−0.81	2.9	28.3	2.8	26.2	60.2
Ag	−0.98	0.0	81.5	0.8	12.4	94.6
Pt	−0.68	0.0	0.0	0.1	95.7	95.8
Au	−0.75	0.0	87.1	0.7	10.2	98.0

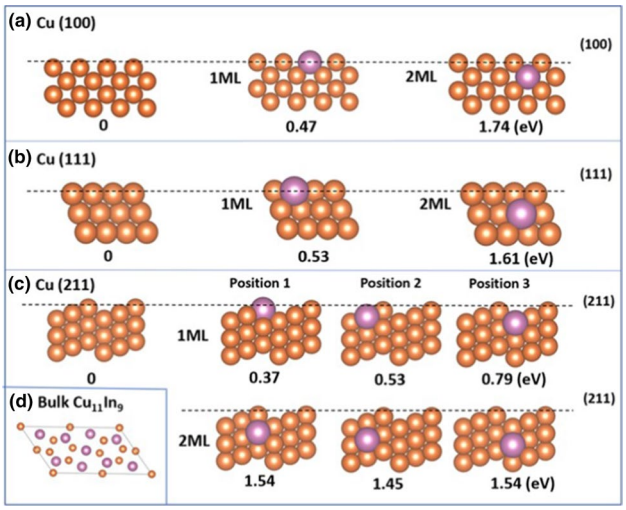

Fig. 4 Side views of **a** Cu(100), **b** C (111) and **c** Cu(211) with a single In atom replacing the first layer (1ML) and second layer (2ML). The energies relative to the pure Cu lattice (pictured left) are presented. **d** Top view of bulk $Cu_{11}In_9$ (adapted from [131])

nanoparticles on catalytic activity in the range ~ 1–8 nm observed a similar trend [141]. On the other hand, for Ag, Pd and Sn nanoparticles, a volcano effect can be observed [139, 142, 143]. For Ag nanoparticles for example, CO_2 reduction current first increased as particle size decreased to 5 nm, below which the reduction current then began to decrease [142]. This volcano effect was suggested to have been related to the binding energy of key intermediates in relation to particle size, however convolution effects may have been at play due to the experiments taking place in ionic liquid electrolyte as opposed to aqueous media.

3.3 Oxide-derived electrocatalysts

Another method of surface morphology engineering has been observed through the oxidation and subsequent reduction of bulk metal catalysts in order to improve catalytic activity [29, 73, 120, 144–146]. Studies on oxide-derived metal catalysts such as Cu, Au and Sn have demonstrated an enhanced density of active sites through the modification of surface structures, leading to improved overpotentials observed for CO_2RR [29, 73, 144]. In a 2012 work by Li et al. [120] conducted on oxide-derived copper (Cu_2O) electrodes observed a coarse surface structure consisting of nanowires, with the reduction activity being strongly dependent on the initial thickness of the Cu_2O layer. The primary products observed from the examined Cu_2O catalysts were formate and CO, produced at both enhanced selectivity and activity. Based on the observed Tafel slope for Cu_2O catalysts, a similar reaction mechanism could be suggested as bulk Cu for the formation of products based on the formation of an activated CO_2 molecule, as observed in Eq. (3), as the rate-determining step. Due to the study focusing on the comparison of geometrical surface area, it would be difficult to conclude as to whether or not the activity of individual catalytic sites was improved without further characterisation with regards to the electrochemically active surface area.

Conversely, for oxide-derived Au, it was found that, as opposed to the nanowire morphology observed for Cu, oxide-derived Au formed a thick layer ($\sim 1\ \mu m$) of nanoparticles [29]. Similarly to oxide-derived Cu, an enhanced faradaic efficiency was, at lower potential, observed for oxide-derived Au when compared with the performance of the bulk metal. This increase in both selectivity and activity was attributed to a higher stability of the reaction intermediate (see Fig. 5). For Au nanoparticles, the enhanced activity has been directly correlated to the density of grain boundaries resulting from the oxidation-reduction step [147, 148].

Oxygen plasma activation has been found to be another form of pre-treatment which results in drastically enhanced CO_2RR activity [33, 149]. Following plasma treatment, the surfaces of oxide-derived metal catalysts were suggested to be defect rich. For plasma treated Cu, both the enhanced reactivity and selectivity have been attributed to the presence of Cu^+ ions and subsurface oxygen. A 2016 work by Eilert et al. [150] suggested that the involvement of subsurface oxygen lead to increased CO binding energies, primarily in the vicinity of grain boundaries. It was believed this was due to its influence on the electronic structure of the catalyst, reducing σ-repulsion. An alternative explanation is that the presence of subsurface oxygen enhances CO_2RR activity by facilitating neutral and charged Cu sites, resulting in in chemisorbed CO_2 in the presence of water [151]. Studies using DFT calculations agree that interstitial oxygen is stable on the Cu fcc(111) surface, unlike the fcc(211) facet, and are capable of improving surface binding of CO_2 [152]. Cavalca

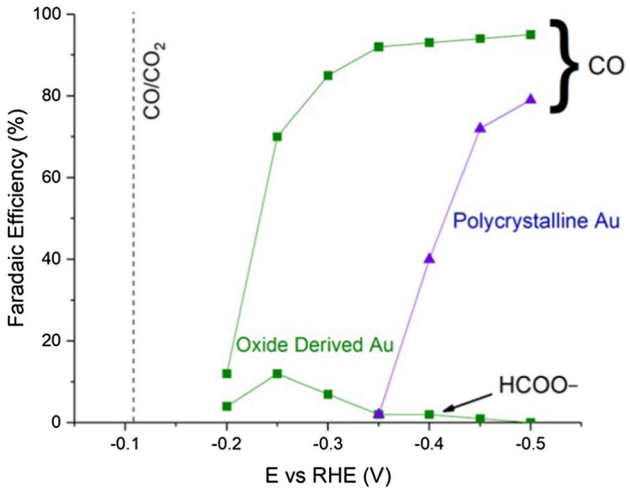

Fig. 5 FEs for CO and HCO_2^- production on oxide-derived Au and polycrystalline Au electrodes at various potentials between − 0.2 and − 0.5 V in 0.5 M $NaHCO_3$, pH 7.2. The dashed line indicates the CO equilibrium potential (adapted from [29])

et al. further supports this hypothesis [153], demonstrating stable sub-surface oxygen present on Cu surfaces for up to 1 h at 1.15 V vs. Reversible hydrogen electrode (RHE). It was further suggested that the presence of subsurface oxygen withdrew charge from the copper sp- and d-bands, selectively enhancing the binding energy of CO. Recent DFT-based work however disputes this, suggesting it unlikely for subsurface oxygen to remain stable at the negative potentials at which CO_2RR takes place due to their low diffusion barriers [154]. A 2018 work by Lum and Ager [155] conducted using ^{18}O labelling similarly concluded that subsurface oxides should indeed be unstable under CO_2RR conditions. Additionally, theoretical work has shown that subsurface oxygen is not a prerequisite for CO_2 adsorption [156] and coordinatively unsaturated Cu atoms promote C–C bond formation [54, 113, 157, 158]. Furthermore, a 2018 work by Fields et al. [154] demonstrated how, from thermodynamic and kinetic perspective, subsurface oxygen should have a negligible effect on the activity of crystalline Cu under reducing potentials.

In short, the role of subsurface oxygen within OD electrocatalysts remains a controversial topic with, as yet, no single agreed solution. Reliable methods capable of measuring, with a certain degree of accuracy, the electrochemically active surface area of metal electrodes [159, 160] will be of paramount importance in once and for all, resolving this ongoing debate of effective surface area effects.

4 Computational methods

Whilst the implementation of Density functional theory (DFT) calculations on the electrode surface can be a complicated affair, a considerable amount of effort has been put into improving models. A recent comprehensive review of such works was produced by Rendòn-Calle et al. [161]. Here we provide a brief review of some of the more fundamental approaches and issues regarding current computational models, in addition to advances in calculating the kinetics of electrochemical steps, structure-sensitive screening, ion effects, and machine learning.

4.1 Kinetic and thermodynamic models

Estimations of catalytic activities based on theoretical calculations have, in recent years, provided fast and increasingly accurate results [24]. By employing DFT and the computational hydrogen electrode model (CHE), calculations can be performed on an atomic scale. This opens up the possibility of screening many novel electrochemical materials and active sites from a thermochemical perspective [162]. The CHE model can be seen discussed in greater detail in Sect. 4.2 however the model has seen widespread use since its creation [163–165].

Through the use of such methods, it has been made feasible to examine possible lowest-overpotential pathways from CO to various C_1 and C_2 products including ethylene, acetaldehyde and ethanol. For any given reaction pathway, the limiting potential U_L is the electrode potential at which all steps are exergonic, i.e. the change in Gibbs energy ΔG is always negative. U_L can be found as the inverse of the largest reaction energy (ΔG_L) [101].

$$U_L = \frac{-\Delta G_L}{e} \tag{7}$$

The first DFT-based studies detailing mechanisms to C_1 species were proposed by Nørskov et al. [166]. By analysing adsorption energies for Cu(100) surfaces, they concluded the lowest energy pathway to be $CO_2 \leftarrow {}^*COOH \leftarrow {}^*CO \leftarrow {}^*CHO \leftarrow {}^*CH_2O \leftarrow {}^*CH_3O \leftarrow CH_4 + {}^*O \leftarrow {}^*OH \leftarrow H_2O$. Using this mechanism, Durand et al. [167] calculated the Gibbs free energies of each reaction intermediate on various Cu facets. Their work found that adsorbates were more easily stabilised on the (211) facet, followed by (100) and (111), in line with simple coordination rules [113, 168–170]. Further studies have since expanded upon this work by examining further Cu facets [171], as well as other transition metals and alloys [172–174].

CO_2RR screening techniques based on scaling relations assuming a single mechanism for all facets and materials however can be further improved [161, 175, 176]. Further information on this can be found in Sect. 4.3. Nie et al. [114, 177], for example, examined the activation barriers for every possible transition state from CO_2 to methane. Based upon their findings, it was discovered that for the Cu(111) facet, *CO is more favourably hydrogenated to *COH rather than *CHO, supporting work performed by Hussain et al. [178]. The pathway continues from here as ${}^*COH \rightarrow {}^*CH \rightarrow {}^*CH_2 \rightarrow {}^*CH_3 \rightarrow CH_4$. A later work by Luo et al. [179] further supports this, demonstrating how unlike the (111) facet, Cu(100) kinetically favours the *CHO pathway over *COH, suggesting a structure-sensitive mechanism dictated by elementary-step kinetics.

Beyond methane formation, thermodynamic studies into the formation of C_2 products such as ethylene (C_2H_4) and ethanol (C_2H_6O) have been explored thermodynamically by Calle-Vallejo and Koper [110]. In their work, the electrochemical reduction of CO (CORR) was studied on Cu(100), considering *CO dimerization as the believed first step toward ethylene, acetaldehyde and ethanol [180]. The electroreduction of CO is contained within CO_2RR, forming a rate limiting step in most CO_2RR reduction processes. The square sites of the Cu(100) facet exhibit strong stabilisation of *CO dimers, helping to explain the Cu(100) facet's preference for ethylene production, whereas step sites tune the product selectivity towards ethanol production [180]. Cheng et al. [157], supports this hypothesis, suggesting in their work that Cu structures with stepped square sites show enhanced selectivity and catalytic activity toward C_2 reaction products. Garza et al. [121] further expanded upon these studies, proposing reaction pathways for all reported C_2 products from CORR (ethylene, ethanol, acetaldehyde, ethylene glycol, glycolaldehyde, glyoxal, and acetate) on both Cu(100) and Cu(111) facets.

The activation energies for C–C bond formation on Cu in vacuum were determined by Montoya et al. [181]. From their work it was found that kinetic barriers depend on the degree of hydrogenation of adsorbates. It was concluded that *CO dimerization is kinetically unfavourable in a vacuum. An initial protonation step of *CO followed by the dimerization of *CHO molecules however, was agreed to be more favourable by comparison. In subsequent work however demonstrated that water-solvated cations stabilize *CO dimers, thus making ${}^*CO \leftarrow {}^*CO$ coupling feasible under CORR conditions, particularly on Cu(100) facets [111].

A key challenge currently facing researchers within catalysis is the formation of multiple C–C bonds, forming C_3 and greater products such as *n*-propanol. Due to the increasing kinetic barriers faced due to the increased complexity of the *n*-propanol molecule, faradaic efficiencies for C_3 products currently remain at consistently low values around 10–13% [127, 182] for *n*-propanol. Small quantities of other C_3 products such as allyl alcohol, acetone, propylene and propane have additionally been observed at low Faradaic efficiencies of $< 3\%$ [31, 182]. Rui et al. suggests that the coupling mechanism for multi-carbon products follows a "polymerisation" scheme of adsorbed CO that obeys the Flory–Schulz distribution [183].

Initial works by Hori performed under strictly galvanostatic conditions ($-5\,\mathrm{mA\,cm^{-2}}$, $\mathrm{E} = -1.1\,\mathrm{V}$ vs. NHE) gave a faradaic efficiency of 4.2% [72, 184]. Under such extreme conditions, Rahaman et al. explains how poor selectivity is a direct result of high overpotentials lowering the required kinetic activation barriers for a variety of competing hydrogenation and C–C coupling processes, particularly those involving *CO [72, 182]. Since then, many strategies aiming to improve product selectivity of CO_2RR have often followed the path of reducing required overpotentials. In his 2017 work Rahaman demonstrates how the addition of a thin oxide "skin" on catalytic surfaces which can be later reduced under CO_2RR conditions [171, 185] can reduce the required overpotentials for C–C bond formation [182]. Such reductions are achieved through the formation of low-coordinated sites from the precursor species, resulting in improved stabilisation of chemisorbed ${}^*CO_2^-$ radical anions, as well as *CO [23]. Such methods were applied to form Cu meshes using annealing and electrodeposition methods to produce catalysts capable of producing *n*-propanol at 13.1% FE at – 1.0V vs. RHE.

Ebaid et al. [186] supports this hypothesis, suggesting surface roughness to be a strong indicator of catalyst performance, as higher surface roughness was attributed to high population of under-coordinated sites. Among the various

methods used to roughen catalyst surfaces, the reduction of Cu_2O [54, 187, 188] and Cu_3N [189] have been shown to be the most effective methods of achieving high selectivity toward C_{2+} products.

C_3 product selectivity however, remains a issue in virtually all Cu-based catalysts [186, 189–192]. Whilst surface roughening methods have shown a drastic improvement in C_3 production, the lack of a controlled or regimented method of surface roughening limits the extent to which structure and activity relationships can be investigated for CO_2RR performance.

4.2 The computational hydrogen electrode (CHE) model

The CHE model is commonly used in the simulation of electrocatalytic systems [162]. It involves the posteriori correction of standard constant charge, allowing for the electrode potential to be taken into account [193]. When utilised in combination with DFT calculations, CHE can provide a picture of the possible reaction pathways and the potentials at which the redox reactions take place [101, 110, 194]. By approximating the equilibrium between protons and electrons with hydrogen, CHE avoids the explicit treatment of the solvated particles like so

$$\frac{1}{2}\mathrm{H}_{2(g)} \leftrightarrow \mathrm{H}^+ + e^-. \tag{8}$$

The chemical potential of a proton–electron pair can therefore be written

$$\frac{1}{2}\mu_{\mathrm{H}_2} = \mu_{(\mathrm{H}^+ + e^-)} \tag{9}$$

where μ_x is the chemical potential of species *x*. For a reductive process, the Gibbs free energy *G* can be related to the electrode potential *U* as

$$\Delta G = -eU \tag{10}$$

thus providing a consistent evaluation of Gibbs energy for all species involved. It should be noted here that *e* is the positive (+) electron charge. The hydrogenation of CO, $^*\mathrm{CO} + \mathrm{H}^+ + e^- \rightarrow {}^*\mathrm{CHO}$ for example, can, for a given potential *U*, be written

$$\Delta G_{^*\mathrm{CO}-^*\mathrm{CHO}} = \mu_{^*\mathrm{CHO}} - \mu_{\mathrm{CO}} - \frac{1}{2}\mu_{\mathrm{H}_2} + eU. \tag{11}$$

Additionally, through the combination of CHE and DFT calculations, one can gain insight into the coverage of surface species at specific pH using a Pourbaix diagram [195]. Works using a combination of both Pourbaix diagrams and CHE can also be found throughout electrochemistry literature [196, 197].

Typically, CHE methods incorporate only CPET steps, however a recent study by Göttle and Koper [78] introduced a method, based on first-principles calculations of acid-base equilibrium constants, which incorporates decoupled proton–electron transfer pathways. Through this, the sequential proton–electron transfer (SPET) pathways can be estimated and provide a computational understanding of pH effects observed experimentally for molecular, metal and oxide-derived catalyst$_2$s [23, 198, 199]. This method has seen use, for example, in rationalising the experimentally determined pH dependence of CO reduction on immobilized cobalt protoporphyrins [79].

4.3 Scaling relations

Scaling relations, i.e. linear correlations between adsorption energies of adsorbates [200], are effective in simplifying DFT-based catalytic models. Through their implementation, scaling relations may impose additional constraints toward further optimising current electrocatalysts. Due to this, scaling relations have been studied extensively [201–203]. Recent works have examined the possibility of breaking scaling relations [113, 204, 205], however breaking such relations has proven to be difficult to achieve experimentally. In order to effectively break scaling relations, one must first stabilise one intermediate with respect to the others. For example, Li et al. [113] explained in their 2014 work how the preference for the producing C_2 products over methane on Cu(100) facets was due to the breaking of scaling relations. They suggest the scaling relations between bound CO and $^*C_2O_2$ on the facet are broken due strong ensemble effects observed during the dimerization step. For CO_2RR, a number of methods

have been discussed within the literature with regards to breaking scaling relations. Alloying, addition of promoters, tethering, the introduction of p-block dopants and creation of low-coordination sites are among some of the strategies which have been suggested throughout the literature [101, 206]. As well as this, some other methods of note are; the alteration of adsorbate solvation via modification of the electrolyte composition/dielectric constant [101, 206], strain effects [207], the study of transition-metal-free catalysts [197] and the anchoring of active ligands on active sites [208].

Conversely, recent studies have shown, based on scaling-relation-based volcano plots, that whilst a single mechanism is operative on all materials and facets [101, 206], the CO_2RR itself is highly sensitive to both structure and material, as previously discussed.

4.4 Effect of structure and pH

pH, structural sensitivity and ion effects are all interconnected during CO_2RR, the interplay of their effects altering reaction mechanisms. Observed onset potentials, faradaic efficiencies and product distributions have been shown to be not only dependant on the chosen catalyst material [23, 209, 210], but also on its surface structure [32, 117]. Typically however, studies based on scaling relation screenings only consider a single reaction mechanism [101, 174, 206]. A work by Calle-Vallejo and Koper [176] however showed that metal- and structure-sensitive bifurcating pathways can be incorporated into screening routines using scaling relations. It should be noted however that breaking scaling relations between *CO and *CHO may lead to enhanced CO_2RR electrocatalysis [101, 206].

In addition to this, it has been observed that both electrolyte pH and local pH effects play an important role in the CO_2RR mechanism. When modelling a system, successive proton-coupled electron transfers are often assumed to take place at every step of the reaction process, so as to enable the use of the CHE model [194]. It should be noted however that the CHE model cannot capture pH effects as the adsorption energies of all intermediates shift proportionally. This problem becomes most apparent when analyzing the CORR due to the strong pH and structure dependent features of the CO intermediate. For example, for pristine Cu, whilst ethene is produced most commonly on the fcc(100) terrace site, CO and methane are more preferentially produced on the fcc(111) facet, both with a strong dependence on pH [209, 211]. A report by Hori [91] suggests the disparity between pH responses indicate that the rate-limiting step of CORR to CH_4 involves proton-coupled electron transfers, making the study of CO_2RR and CORR to CH_4 suitable for CHE models. The formation of C_2H_4 however does not include such reactions, and should be analyzed cautiously.

In a 1991 work by Murata et al. [212], it was shown that the production of multi-carbon species could be enhanced through the use of alkaline cations. The selectivity toward C_2H_4, for example, can be increased by the inclusion of larger cations as their smaller hydration spheres better favour adsorption on cathodic surfaces, yielding more positive potential values. Singh et al. [213] explained cation effects based on the pk_a values for their hydrolysis. The larger CO_2 concentrations near the cathode and lower local pH observed with increasing cation size both being satisfactorily explaining cation effects for the CO_2RR but not those observed for the CORR.

When factoring-in cation effects into computational models, cation effects may be included implicitly or explicitly. For example, one study by Chen et al. [214] used an implicit method of modelling cation effects, applying a general electric field as opposed to individual point charges. The electric field then interacts with adsorbates, modifying the adsorption energies depending on the on the dipole moment of a given species [215]. Conversely, Akhade et al. [216], used an explicit model of cation effects in combination with DFT calculations to account for the impact of adsorbed and co-adsorbed I^- and K^+ ion, on *CO protonation. Through this work it was found that K^* improves *CO and *CHO binding over *COH, improving the selectivity toward the *CHO pathway. By contrast, I^* weakens the binding energy of *CO, *COH and *CHO, resulting in an improved selectivity toward the formation CO as the primary reduction product. In later works, it was suggested that specific halide adsorption on Cu may occur at negative electrode potentials [179]. As a consequence of this, it was found that the specific adsorption of Cl^-, Br^-, and I^- affect the CO_2RR. A 2016 work by Vaela et al. [217] supports these results. Their experimental observations showing a 3.5 times higher selectivity toward CO production using Br^- as opposed to Cl^-, as well as I^- favouring the reduction of CO to methane over CO desorption. Perez-Gallent et al. [122] presented a joint computational-experimental study on the impact of cation effects on CORR. Using an explicit model, it was observed that hydrogenation of monomers was particularly more difficult than that of dimers. This was attributed to the fact that cations stabilize C_2 adsorbates but not C_1 intermediates. This discovery could explain why C_2H_4 exhibits earlier onset potentials than CH_4 [122].

4.5 Machine learning

Computational works fully based upon DFT calculations for CO_2RR providing a comprehensive amount of detail for the catalytic activity of materials. such works however are often computationally expensive. In addition to the study of scaling relations, machine learning algorithms offer an alternative approach toward electrocatalyst selection and design. By using an extensive library of preexisting data from previous research, trends within previously documented results are detected and examined during an initial "training phase". Following this, provided suitable descriptors have been selected, a process of statistical analyses can be used to predict, within a degree of accuracy, new materials selective toward a desired product without performing new DFT calculations [218, 219].

One such machine learning framework, for example, was presented by Ulissi et al. [220]. Through this framework, they examined numerous configurations and active sites on intermetallic compounds. The results of their method explained the activity of certain NiGa sites and suggested the need for a composition-, configuration- and structure-sensitive methods to speed up the discovery of new catalytic materials. Research conducted by Jiang et al. used genetic algorithms to find stable solid-liquid interfaces on Cu to account for solvation effects when modelling CORR [221]. Similarly, Xin et al. used a neural network-based chemisorption model in tandem with scaling relations to predict CO_2RR to C_2 reaction products on $(100-)$ terminated catalysts [222]. One such work by Zhong et al. [223], developed a machine learning accelerated, high-throughput DFT framework allowing for new materials to be screened ab-initio. Through this particular work, Zhong et al. discovered a promising bi-metallic CuAl compound with near optimal CO adsorption energy (-0.67 eV) with an observed faradaic efficiency of $\sim 80\%$ with a partial current density of $600\ \mathrm{mA\ cm^{-2}}$.

Despite the tremendous potential of machine-learning algorithms, their predictive capabilities depend largely on the size and quality of the training dataset, as well as the descriptor of choice. For example, assuming a single mechanism for all materials, datasets made of unrelaxed calculations and similar simplifications can lead to incorrect predictions [219].

To summarise, significant progress has been made in the development of computational models, however a number of challenges must be overcome in order to develop more accurate screening routines for the design of CO_2 and CO reduction materials [175].

5 Conclusion

The reduction of CO_2 to multi-carbon products such as hydrocarbons consists of multiple complex reaction steps involving many shared intermediates depending on the desired reaction product. In recent decades, a significant amount of progress has been made regarding the design of highly active or selective electrocatalysts, particularly for the formation of CO and formate. For the formation of larger products involving multiple carbon atoms such as ethylene however, a greater understanding of the reaction mechanisms is required. In particular, improving understanding of key areas such as the effect of the electrode surface morphology on product selectivity, sub-surface structure as well as the effect of local pH. Now, due to a lack of effective probes able to examine quantities outside macroscopic equilibria, a combination of both experimental and computational methods could provide the key to developing a greater understanding of the reaction phenomena taking place. In terms of computational modelling of electrocatalysts, one possible method of improving the understanding of a system could be through combining numerous theoretical models to develop beyond the specific cases which certain models are tuned toward. This would require both a more standardised approach toward future experimental setups, as well as a conscious effort to develop future computational models beyond merely the surface characteristics of potential catalyst designs. Even after 35 years of research, there is still much work to be done, particularly in the development of catalysts more selective toward the production of liquid fuels. The "one-pot" synthesis of chemicals from waste CO_2 however, particularly fuels, represents a useful and potentially game-changing method of moving toward a carbon neutral future with minimal impact on existing infrastructure.

Authors' contributions SR conceived the project. IB constructed the framework of the manuscript and summarized the literature. All the authors were involved in writing the manuscript. All authors read and approved the final manuscript.

Funding This work was supported by the Engineering and Physical Sciences Research Council [Grant Number EP/S023836/1].

Data availability All data analysed during this review paper is within the article.

Code availability Not applicable.

Declarations

Ethics approval and consent to participate Not applicable.

Competing interests The authors declare no competing interests.

References

1. Ritchie H. Energy. Our world in data; 2014. https://ourworldindata.org/energy.
2. Ritchie H. Fossil fuels. Our world in data; 2017. https://ourworldindata.org/fossil-fuels.
3. Olah GA, Goeppert A, Surya Prakash GK. Chemical recycling of carbon dioxide to methanol and dimethyl ether: from greenhouse gas to renewable, environmentally carbon neutral fuels and synthetic hydrocarbons. J Org Chem. 2009;74(2):487–98.
4. Carlson KM, Gerber JS, Mueller ND, Herrero M, MacDonald GK, Brauman KA, Havlik P, O'Connell CS, Johnson JA, Saatchi S, West PC. Greenhouse gas emissions intensity of global croplands. Nat Clim Change. 2017;7(1):63–8.
5. Mohammed SJ, Mansoori GA. A unique view on carbon dioxide emissions around the world. Glob J Earth Sci Eng. 2017;4(1):8–17.
6. Lewis NS, Nocera DG. Powering the planet: chemical challenges in solar energy utilization. Proc Natl Acad Sci. 2006;103(43):15729–35.
7. Olah GA. Beyond oil and gas: the methanol economy. Angew Chem Int Ed. 2005;44(18):2636–9.
8. Fuqiang W, Ziming C, Jianyu T, Yuan Y, Yong S, Linhua L. Progress in concentrated solar power technology with parabolic trough collector system: a comprehensive review. Renew Sustain Energy Rev. 2017;79(C):1314–28.
9. Korkas C, Baldi S, Michailidis I, Kosmatopoulos E. Occupancy-based demand response and thermal comfort optimization in microgrids with renewable energy sources and energy storage. Appl Energy. 2016;163:93–104, 02.
10. Muhich CL, Ehrhart BD, Al-Shankiti I, Ward BJ, Musgrave CB, Weimer AW. A review and perspective of efficient hydrogen generation via solar thermal water splitting. WIREs Energy Environ. 2016;5(3):261–87.
11. Jiang C, Moniz SJA, Wang A, Zhang T, Tang J. Photoelectrochemical devices for solar water splitting—materials and challenges. Chem Soc Rev. 2017;46(15):4645–60.
12. Kumar B, Brian JP, Atla V, Kumari S, Bertram KA, White RT, Spurgeon JM. New trends in the development of heterogeneous catalysts for electrochemical CO_2 reduction. Catal Today. 2016;270:19–30.
13. Theaker N, Strain JM, Bijandra Kumar J, Brian P, Kumari S, Spurgeon JM. Heterogeneously catalyzed two-step cascade electrochemical reduction of CO_2 to ethanol. Electrochim Acta. 2018;274:1–8.
14. White JL, Herb JT, Kaczur JJ, Majsztrik PW, Bocarsly AB. Photons to formate: efficient electrochemical solar energy conversion via reduction of carbon dioxide. J CO_2 Util. 2014;7:1–5.
15. Whipple DT, Kenis PJA. Prospects of CO_2 utilization via direct heterogeneous electrochemical reduction. J Phys Chem Lett. 2010;1(24):3451–8.
16. Centi G, Perathoner S. Opportunities and prospects in the chemical recycling of carbon dioxide to fuels. Catal Today. 2009;148:191–205, 11.
17. Durst J, Rudnev A, Dutta A, Yongchun F, Herranz J, Kaliginedi V, Kuzume A, Permyakova AA, Paratcha Y, Broekmann P, Schmidt TJ. Electrochemical CO_2 reduction—a critical view on fundamentals, materials and applications. Chimia. 2015;69(12):769–76.
18. Jones JP, Surya Prakash GK, Olah GA. Electrochemical CO_2 reduction: recent advances and current trends. Israel J Chem. 2014;54(10):1451–66.
19. Zuman P. Modern aspects of electro-chemistry. Adv Coll Interface Sci. 1981;14(4):282–3.
20. Birdja YY, Pérez-Gallent E, Figueiredo MC, Göttle AJ, Calle-Vallejo F, Koper MTM. Advances and challenges in understanding the electrocatalytic conversion of carbon dioxide to fuels. Nat Energy. 2019;4(9):732–45.
21. Hori Y. Electrochemical CO_2 reduction on metal electrodes. In: Modern aspects of electrochemistry. New York: Springer; 2008. p. 101.
22. Ibram G. Conversion of carbon dioxide into methanol—a potential liquid fuel: fundamental challenges and opportunities (a review). Renew Sustain Energy Rev. 2014;31:221–57.
23. Kortlever R, Shen J, Klaas JP, Schouten FC-V, Koper MTM. Catalysts and reaction pathways for the electrochemical reduction of carbon dioxide. J Phys Chem Lett. 2015;6(20):4073–82.
24. Seh ZW, Kibsgaard J, Dickens CF, Chorkendorff IB, Nørskov JK, Jaramillo TF. Combining theory and experiment in electrocatalysis: insights into materials design. Science. 2017;355(6321):eaad4998.
25. Hori Y, Wakebe HHI, Tsukamoto T, Koga O. Electrocatalytic process of CO selectivity in electrochemical reduction of CO_2 at metal electrodes in aqueous media. Electrochim Acta. 1994;39(11–12):1833–9.
26. Min X, Kanan MW. Pd-catalyzed electrohydrogenation of carbon dioxide to formate: high mass activity at low overpotential and identification of the deactivation pathway. J Am Chem Soc. 2015;137(14):4701–8.

27. Kortlever R, Peters I, Koper S, Koper MTM. Electrochemical CO_2 reduction to formic acid at low overpotential and with high faradaic efficiency on carbon-supported bimetallic Pd–Pt nanoparticles. ACS Catal. 2015;5(7):3916–23.
28. Cave ER, Montoya JH, Kuhl KP, Abram DN, Hatsukade T, Shi C, Hahn C, Nørskov JK, Jaramillo TF. Electrochemical CO_2 reduction on Au surfaces: mechanistic aspects regarding the formation of major and minor products. Phys Chem Chem Phys. 2017;19(24):15856–63.
29. Chen Y, Li CW, Kanan MW. Aqueous CO_2 reduction at very low overpotential on oxide-derived au nanoparticles. J Am Chem Soc. 2012;134(49):19969–72.
30. Hatsukade T, Kuhl KP, Cave ER, Abram DN, Jaramillo TF. Insights into the electrocatalytic reduction of CO_2 on metallic silver surfaces. Phys Chem Chem Phys. 2014;16(27):13814–9.
31. Kuhl KP, Cave ER, Abram DN, Jaramillo TF. New insights into the electrochemical reduction of carbon dioxide on metallic copper surfaces. Energy Environ Sci. 2012;5(5):7050–9.
32. Hori Y, Takahashi I, Koga O, Hoshi N. Electrochemical reduction of carbon dioxide at various series of copper single crystal electrodes. J Mol Catal A Chem. 2003;199(1–2):39–47.
33. Mistry H, Varela AS, Bonifacio CS, Zegkinoglou I, Sinev I, Choi YW, Kisslinger K, Stach EA, Yang JC, Strasser P, Cuenya BR. Highly selective plasma-activated copper catalysts for carbon dioxide reduction to ethylene. Nat Commun. 2016;7:1–9.
34. Yano H, Tanaka T, Nakayama M, Ogura K. Selective electrochemical reduction of CO_2 to ethylene at a three-phase interface on copper(I) halide-confined Cu-mesh electrodes in acidic solutions of potassium halides. J Electroanal Chem. 2004;565(2):287–93.
35. Dinh CT, Burdyny T, Kibria MG, Seifitokaldani A, Gabardo CM, García de Arquer FP, Kiani A, Edwards JP, De Luna P, Bushuyev OS, Zou C. CO_2 electroreduction to ethylene via hydroxide-mediated copper catalysis at an abrupt interface. Science. 2018;360(6390):783–7.
36. Payra S, Shenoy S, Chakraborty C, Tarafder K, Roy S. Structure-sensitive electrocatalytic reduction of CO_2 to methanol over carbon-supported intermetallic PtZn nano-alloys. ACS Appl Mater Interfaces. 2020;12(17):19402–14.
37. Huang J, Guo X, Yue G, Qiong H, Wang L. Boosting CH_3 OH production in electrocatalytic CO_2 reduction over partially oxidized 5 nm cobalt nanoparticles dispersed on single-layer nitrogen-doped graphene. ACS Appl Mater Interfaces. 2018;10(51):44403–14.
38. Ren D, Deng Y, Handoko AD, Chen CS, Malkhandi S, Yeo BS. Selective electrochemical reduction of carbon dioxide to ethylene and ethanol on copper(I) oxide catalysts. ACS Catal. 2015;5(5):2814–21.
39. Chi D, Yang H, Yanfang D, Lv T, Sui G, Wang H, Jiaxing L. Morphology-controlled CuO nanoparticles for electroreduction of CO_2 to ethanol. RSC Adv. 2014;4(70):37329–32.
40. Song Y, Peng R, Hensley DK, Bonnesen PV, Liang L, Zili W, Meyer HM, Chi M, Ma C, Sumpter BG, Rondinone AJ. High-selectivity electrochemical conversion of CO_2 to ethanol using a copper nanoparticle/N-doped graphene electrode. ChemistrySelect. 2016;1(19):6055–61.
41. Saito M. R&D activities in Japan on methanol synthesis from CO_2 and H_2. Catal Surv Jpn. 1998;2(2):175–84.
42. Saito M, Takeuchi M, Watanabe T, Toyir J, Luo S, Wu J. Methanol synthesis from CO_2 and H_2 over a CuZnO-based multicomponent catalyst. Energy Convers Manag. 1997;38:S403–8.
43. Bartholomew CH, Farrauto RJ. Hydrogen production and synthesis gas reactions. In: Fundamentals of industrial catalytic processes. Hoboken: Wiley; 2006. p. 339–486.
44. Behrens M, Studt F, Kasatkin I, Kühl S, Hävecker M, Abild-Pedersen F, Zander S, Girgsdies F, Kurr P, Kniep B-L, et al. The active site of methanol synthesis over $Cu/ZnO/Al_2O_3$ industrial catalysts. Science. 2012;336(6083):893–7.
45. Russell WW, Miller GH. Catalytic hydrogenation of carbon dioxide to higher hydrocarbons. J Am Chem Soc. 1950;72(6):2446–54.
46. Dorner RW, Hardy DR, Williams FW, Willauer HD. Heterogeneous catalytic CO_2 conversion to value-added hydrocarbons. Energy Environ Sci. 2010;3(7):884–90.
47. Wang B, Li Y, Nan W, Lan CQ. CO_2 bio-mitigation using microalgae. Appl Microbiol Biotechnol. 2008;79(5):707–18.
48. Yaashikaa PR, Senthil Kumar P, Varjani Sunita J, Saravanan A. A review on photochemical, biochemical and electrochemical transformation of CO_2 into value-added products. J CO_2 Util. 2019;33(1):131–47.
49. Kumar B, Llorente M, Froehlich J, Dang T, Sathrum A, Kubiak CP. Photochemical and photoelectrochemical reduction of CO_2. Annu Rev Phys Chem. 2012;63(1):541–69.
50. Morris AJ, Meyer GJ, Fujita E. Molecular approaches to the photocatalytic reduction of carbon dioxide for solar fuels, accounts of chemical research. Acc Chem Res. 2009;42(12):1983–94.
51. Li K, An X, Park KH, Khraisheh M, Tang J. A critical review of CO_2 photoconversion: catalysts and reactors. Catal Today. 2014;224:3–12.
52. Umeda M, Niitsuma Y, Horikawa T, Matsuda S, Osawa M. Electrochemical reduction of CO_2 to hydrocarbons to store renewable electrical energy and upgrade biogas. Energy Convers Manag. 2007;48(4):1255–65.
53. Zhong S, Cao Z, Yang X, Kozlov SM, Huang KW, Tung V, Cavallo L, Li LJ, Han Y. Electrochemical conversion of CO_2 to 2-bromoethanol in a membraneless cell. ACS Energy Lett. 2019;4(2):600–5.
54. Jiang K, Sandberg RB, Akey AJ, Liu X, Bell DC, Nørskov JK, Chan K, Wang H. Metal ion cycling of Cu foil for selective C–C coupling in electrochemical CO_2 reduction. Nat Catal. 2018;1(2):111–9.
55. Yao B, Xiao T, Makgae OA, Jie X, Gonzalez-Cortes S, Guan S, Kirkland AI, Dilworth JR, Al-Megren HA, Alshihri SM, Dobson PJ. Transforming carbon dioxide into jet fuel using an organic combustion-synthesized Fe–Mn–K catalyst. Nat Commun. 2020;11(1):1–12.
56. Verma S, Hamasaki Y, Kim C, Huang W, Lu S, Jhong HR, Gewirth AA, Fujigaya T, Nakashima N, Kenis PJ. Insights into the low overpotential electroreduction of CO_2 to CO on a supported gold catalyst in an alkaline flow electrolyzer. ACS Energy Lett. 2018;3(1):193–8.
57. De Luna P, Hahn C, Higgins D, Jaffer SA, Jaramillo TF, Sargent EH. What would it take for renewably powered electrosynthesis to displace petrochemical processes? Science. 2020;350(3):eaav3506.
58. Tascedda P, Weidmann M, Dinjus E, Duach E. Recent developments in electrochemical and photoelectrochemical CO_2 reduction: involvement of the $(CO_2)2^{\cdot-}$ dimer radical anion. Appl Organomet Chem. 2001;15(2):113–20.
59. Rosen BA, Salehi-Khojin A, Thorson MR, Zhu W, Whipple DT, Kenis PJ, Masel RI. Ionic liquid-mediated selective conversion of CO_2 to co at low overpotentials. Science. 2011;334(6056):643–4.
60. Benson EE, Kubiak CP, Sathrum AJ, Smieja JM. Electrocatalytic and homogeneous approaches to conversion of CO_2 to liquid fuels. Chem Soc Rev. 2009;38(1):89–99.
61. Chandrasekaran K, Bockris LM. In-situ spectroscopic investigation of adsorbed intermediate radicals in electrochemical reactions: CO_2^- on platinum. Surf Sci. 1987;185(3):495–514.

62. Bockris JOM, Wass JC. On the photoelectrocatalytic reduction of carbon dioxide. Mater Chem Phys. 1989;22(3–4):249–80.
63. Delacourt C, Ridgway PL, Newman J. Mathematical modeling of CO_2 reduction to CO in aqueous electrolytes. J Electrochem Soc. 2010;157(12):B1902.
64. Lee CH, Kanan MW. Controlling H+ vs CO_2 reduction selectivity on Pb electrodes. ACS Catal. 2015;5(1):465–9.
65. Del Castillo A, Alvarez-Guerra M, Solla-Gullón J, Sáez A, Montiel V, Irabien A. Sn nanoparticles on gas diffusion electrodes: synthesis, characterization and use for continuous CO_2 electroreduction to formate. J CO_2 Util. 2017;18:222–8.
66. Zhang X, Lei T, Liu Y, Qiao J. Enhancing CO_2 electrolysis to formate on facilely synthesized Bi catalysts at low overpotential. Appl Catal B. 2017;218:46–50.
67. Kim S, Dong WJ, Gim S, Sohn W, Park JY, Yoo CJ, Jang HW, Lee JL. Shape-controlled bismuth nanoflakes as highly selective catalysts for electrochemical carbon dioxide reduction to formate. Nano Energy. 2017;39(May):44–52.
68. Rabiee A, Nematollahi D. Electrochemical reduction of CO_2 to formate ion using nanocubic mesoporous In(OH)3/carbon black system. Mater Chem Phys. 2017;193:109–16.
69. Gattrell M, Gupta N, Co A. A review of the aqueous electrochemical reduction of CO_2 to hydrocarbons at copper. J Electroanal Chem. 2006;594(1):1–19.
70. Singh MR, Goodpaster JD, Weber AZ, Head-Gordon M, Bell AT. Mechanistic insights into electrochemical reduction of CO_2 over Ag using density functional theory and transport models. Proc Natl Acad Sci USA. 2017;114(42):E8812–21.
71. Bagger A, Ju W, Varela AS, Strasser P, Rossmeisl J. Electrochemical CO_2 reduction: a classification problem. ChemPhysChem. 2017;18(22):3266–73.
72. Hori Y, Murata A, Takahashi R. Formation of hydrocarbons in the electrochemical reduction of carbon dioxide at a copper electrode in aqueous solution. J Chem Soc Faraday Trans 1. 1989;85:2309–26.
73. Chen Y, Kanan MW. Tin oxide dependence of the CO_2 reduction efficiency on tin electrodes and enhanced activity for tin/tin oxide thin-film catalysts. J Am Chem Soc. 2012;134(4):1986–9.
74. Luc W, Collins C, Wang S, Xin H, He K, Kang Y, Jiao F. Ag-–Sn bimetallic catalyst with a core-shell structure for CO_2 reduction. J Am Chem Soc. 2017;139(5):1885–93.
75. Baruch MF, Pander III JE, White JL, Bocarsly AB. Mechanistic insights into the reduction of CO_2 on tin electrodes using in situ ATR-IR spectroscopy. ACS Catal. 2015;5(5):3148–56.
76. Scholten F, Nguyen K-LC, Bruce JP, Heyde M, Cuenya BR. Identifying structure-selectivity correlations in the electrochemical reduction of CO_2: a comparison of well-ordered atomically clean and chemically etched copper single-crystal surfaces. Angew Chem Int Ed. 2021;60(35):19169–75.
77. Yoo JS, Christensen R, Vegge T, Nørskov JK, Studt F. Theoretical insight into the trends that guide the electrochemical reduction of carbon dioxide to formic acid. ChemSusChem. 2016;9(4):358–63.
78. Göttle AJ, Koper MTM. Proton-coupled electron transfer in the electrocatalysis of CO_2 reduction: prediction of sequential vs. concerted pathways using DFT. Chem Sci. 2016;8(1):458–65.
79. Shen J, Kortlever R, Kas R, Birdja YY, Diaz-Morales O, Kwon Y, Ledezma-Yanez I, Schouten KJ, Mul G, Koper M. Electrocatalytic reduction of carbon dioxide to carbon monoxide and methane at an immobilized cobalt protoporphyrin. Nat Commun. 2015;6(1):1–8.
80. Shen J, Kolb MJ, Göttle AJ, Koper MTM. DFT study on the mechanism of the electrochemical reduction of CO_2 catalyzed by cobalt porphyrins. J Phys Chem C. 2016;120(29):15714–21.
81. Koper MTM. Theory of the transition from sequential to concerted electrochemical proton–electron transfer. Phys Chem Chem Phys. 2013;15(5):1399–407.
82. Monteiro MCO, Dattila F, Hagedoorn B, García-Muelas R, López N, Koper M. Absence of CO_2 electroreduction on copper, gold and silver electrodes without metal cations in solution. Nat Catal. 2021;4(8):654–62.
83. Birdja YY, Shen J, Koper MTM. Influence of the metal center of metalloprotoporphyrins on the electrocatalytic CO_2 reduction to formic acid. Catal Today. 2017;288:37–47.
84. Hori Y. Electrochemical CO_2 reduction on metal electrodes. New York: Springer; 2008. p. 89–189.
85. Azuma M. Electrochemical reduction of carbon dioxide on various metal electrodes in low-temperature aqueous $KHCO_3$ media. J Electrochem Soc. 1990;137(6):1772.
86. Solis BH, Maher AG, Dogutan DK, Nocera DG, Hammes-Schiffer S. Nickel phlorin intermediate formed by proton-coupled electron transfer in hydrogen evolution mechanism. Proc Natl Acad Sci USA. 2016;113(3):485–92.
87. Göttle AJ, Koper MTM. Determinant role of electrogenerated reactive nucleophilic species on selectivity during reduction of CO_2 catalyzed by metalloporphyrins. J Am Chem Soc. 2018;140(14):4826–34.
88. Loewen ND, Neelakantan TV, Berben LA. Renewable formate from C–H bond formation with CO_2: using iron carbonyl clusters as electrocatalysts. Acc Chem Res. 2017;50(9):2362–70.
89. Tang Q, Lee Y, Li DY, Choi W, Liu CW, Lee D, Jiang DE. Lattice-hydride mechanism in electrocatalytic CO_2 reduction by structurally precise copper-hydride nanoclusters. J Am Chem Soc. 2017;139(28):9728–36.
90. Groenenboom MC, Keith JA. Quantum chemical analyses of BH_4^- and BH_3OH^- hydride transfers to CO_2 in aqueous solution with potentials of mean force. ChemPhysChem. 2017;18(22):3148–52.
91. Hori Y, Takahashi R, Yoshinami Y, Murata A. Electrochemical reduction of CO at a copper electrode. J Phys Chem B. 1997;101(36):7075–81.
92. Varela AS. The importance of pH in controlling the selectivity of the electrochemical CO_2 reduction. Curr Opin Green Sustain Chem. 2020;26:11.
93. Haag MR. Handbook of chemistry. Agron J. 1950;42(2):111–2.
94. Lim RJ, Xie M, Sk MA, Lee JM, Fisher A, Wang X, Lim KH. A review on the electrochemical reduction of CO_2 in fuel cells, metal electrodes and molecular catalysts. Catal Today. 2014;233:169–180.
95. Prieto G. Carbon dioxide hydrogenation into higher hydrocarbons and oxygenates: thermodynamic and kinetic bounds and progress with heterogeneous and homogeneous catalysis. Chemsuschem. 2017;10(6):1056–70.
96. Hori Y, Murata A, Yoshinami Y. Adsorption of CO, intermediately formed in electrochemical reduction of CO_2, at a copper electrode. J Chem Soc Faraday Trans. 1991;87(1):125–8.

97. Hori Y, Murata A, Tsukamoto T, Wakebe H, Koga O, Yamazaki H. Adsoprtion of carbon monoxide at a copper electrode accompanied by electron transfer observed by voltammetry and IR spectroscopy. Electrochim Acta. 1994;39(17):2495–500.
98. Production at, metal of, electrochemical reduction, of CO, Chiba Hori, Synthetic Katsuhei Kikuchi, Faculty Chiba Shin, and Suzuki Engineering. The chemicals. Laboratory Techniques in Biochemistry and Molecular Biology. 1990;20(C):5–51.
99. Vielstich W, Lamm A, Gasteiger HA. Materials and manufacturing processes. In: Reitz W, editor. Handbook of fuel cells: fundamentals, technology, and applications (Volume 2). Hoboken: Wiley; 2007. p. 789.
100. Hara K, Kudo A, Sakata T. Electrochemical reduction of high pressure carbon dioxide on Fe electrodes at large current density. J Electroanal Chem. 1995;386(1–2):257–60.
101. Peterson AA, Nørskov JK. Activity descriptors for CO_2 electroreduction to methane on transition-metal catalysts. J Phys Chem Lett. 2012;3(2):251–8.
102. Torelli DA, Francis SA, Crompton JC, Javier A, Thompson JR, Brunschwig BS, Soriaga MP, Lewis NS. Nickel-gallium-catalyzed electrochemical reduction of CO_2 to highly reduced products at low overpotentials. ACS Catal. 2016;6(3):2100–4.
103. Kortlever R, Peters I, Balemans C, Kas R, Kwon Y, Mul G, Koper MTM. Palladium-gold catalyst for the electrochemical reduction of CO_2 to C1–C5 hydrocarbons. Chem Commun. 2016;52(67):10229–32.
104. Calvinho KU, Alherz AW, Yap KM, Laursen AB, Hwang S, Bare ZJ, Clifford Z, Musgrave CB, Dismukes GC. Selective CO_2 reduction to C3 and C4 oxyhydrocarbons on nickel phosphides at overpotentials as low as 10 mV. Energy Environ Sci. 2018;11(9):2550–9.
105. Fan Q, Zhang M, Jia M, Liu S, Qiu J, Sun Z. Electrochemical CO_2 reduction to C2+ species: heterogeneous electrocatalysts, reaction pathways, and optimization strategies. Mater Today Energy. 2018;10:280–301.
106. Han Z, Kortlever R, Chen HY, Peters JC, Agapie T. CO_2 reduction selective for $C \geq 2$ products on polycrystalline copper with N-substituted pyridinium additives. ACS Cent Sci. 2017;3(8):853–9.
107. Hoang TT, Verma S, Ma S, Fister TT, Timoshenko J, Frenkel AI, Kenis PJ, Gewirth AA. Nanoporous copper–silver alloys by additive-controlled electrodeposition for the selective electroreduction of CO_2 to ethylene and ethanol. J Am Chem Soc. 2018;140(17):5791–7.
108. Gao D, McCrum IT, Deo S, Choi YW, Scholten F, Wan W, Chen JG, Janik MJ, Roldan Cuenya B. Activity and selectivity control in CO_2 electroreduction to multicarbon products over CuOx catalysts via electrolyte design. ACS Catal. 2018;8(11):10012–20.
109. Bushuyev OS, De Luna P, Dinh CT, Tao L, Saur G, van de Lagemaat J, Kelley SO, Sargent EH. What should we make with CO_2 and how can we make it? Joule. 2018;2(5):825–32.
110. Calle-Vallejo F, Koper MT. Theoretical considerations on the electroreduction of CO to C2 species on Cu(100) electrodes. Angew Chem Int Ed. 2013;52(28):7282–5.
111. Montoya JH, Shi C, Chan K, Nørskov JK. Theoretical insights into a CO dimerization mechanism in CO_2 electroreduction. J Phys Chem Lett. 2015;6(11):2032–7.
112. Goodpaster JD, Bell AT, Head-Gordon M. Identification of possible pathways for C–C bond formation during electrochemical reduction of CO_2: new theoretical insights from an improved electrochemical model. J Phys Chem Lett. 2016;7(8):1471–7.
113. Li H, Li Y, Koper MT, Calle-Vallejo F. Bond-making and breaking between carbon, nitrogen, and oxygen in electrocatalysis. J Am Chem Soc. 2014;136(44):15694–701.
114. Nie X, Esopi MR, Janik MJ, Asthagiri A. Selectivity of CO_2 reduction on copper electrodes: the role of the kinetics of elementary steps. Angew Chem Int Ed. 2013;52(9):2459–62.
115. Schouten KJP, Kwon Y, Van Der Ham CJM, Qin Z, Koper MTM. A new mechanism for the selectivity to C1 and C2 species in the electrochemical reduction of carbon dioxide on copper electrodes. Chem Sci. 2011;2(10):1902–9.
116. Schouten KJ, Pérez Gallent E, Koper MT. Structure sensitivity of the electrochemical reduction of carbon monoxide on copper single crystals. ACS Catal. 2013;3(6):1292–5.
117. Schouten KJ, Qin Z, Pérez Gallent E, Koper MT. Two pathways for the formation of ethylene in CO reduction on single-crystal copper electrodes. J Am Chem Soc. 2012;134(24):9864–7.
118. Wuttig A, Liu C, Peng Q, Yaguchi M, Hendon CH, Motobayashi K, Ye S, Osawa M, Surendranath Y. Tracking a common surface-bound intermediate during CO_2-to-fuels catalysis. ACS Cent Sci. 2016;2(8):522–8.
119. Hori Y, Murata A, Takahashi R, Suzuki S. Electroreduction of CO to CH4 and C2H4 at a copper electrode in aqueous solutions at ambient temperature and pressure. J Am Chem Soc. 1987;109(16):5022–3.
120. Li CW, Kanan MW. CO_2 reduction at low overpotential on Cu electrodes resulting from the reduction of thick Cu_2O films. J Am Chem Soc. 2012;134(17):7231–4.
121. Garza AJ, Bell AT, Head-Gordon M. Mechanism of CO_2 reduction at copper surfaces: pathways to C2 products. ACS Catal. 2018;8(2):1490–9.
122. Pérez-Gallent E, Figueiredo MC, Calle-Vallejo F, Koper MT. Spectroscopic observation of a hydrogenated CO dimer intermediate during CO reduction on Cu(100) electrodes. Angew Chem Int Ed. 2017;56(13):3621–4.
123. Wang X, Wang Z, Zhuang T-T, Dinh C-T, Li J, Nam D-H, Li F, Huang C-W, Tan C-S, Chen Z, Chi M, Gabardo CM, Seifitokaldani A, Todorović P, Proppe A, Pang Y, Kirmani AR, Wang Y, Ip AH, Richter LJ, Scheffel B, Aoni X, Lo S-C, Kelley SO, Sinton D, Sargent EH. Efficient upgrading of CO to C3 fuel using asymmetric C–C coupling active sites. Nat Commun. 2019;10(1):5186.
124. Bagger A, Ju W, Varela AS, Strasser P, Rossmeisl J. Electrochemical CO_2 reduction: classifying cu facets. ACS Catal. 2019;9(9):7894–9.
125. Xiao H, Cheng T, Goddard WA. Atomistic mechanisms underlying selectivities in C1 and C2 products from electrochemical reduction of CO on Cu(111). J Am Chem Soc. 2017;139(1):130–6.
126. Zhuang TT, Pang Y, Liang ZQ, Wang Z, Li Y, Tan CS, Li J, Dinh CT, De Luna P, Hsieh PL, Burdyny T, et al. Copper nanocavities confine intermediates for efficient electrosynthesis of C3 alcohol fuels from carbon monoxide. Nat Catal. 2018;1(12):946–51.
127. Ren D, Wong NT, Handoko AD, Huang Y, Yeo BS. Mechanistic insights into the enhanced activity and stability of agglomerated Cu nanocrystals for the electrochemical reduction of carbon dioxide to *n*-propanol. J Phys Chem Lett. 2016;7(1):20–4.
128. Tang MT, Peng HJ, Stenlid JH, Abild-Pedersen F. Exploring trends on coupling mechanisms toward C3 product formation in CO(2)R. J Phys Chem C. 2021;125(48):26437–47.
129. Hao J, Shi W. Transition metal (Mo, Fe Co, and Ni)-based catalysts for electrochemical CO_2 reduction. Cuihua Xuebao/Chin J Catal. 2018;39(7):1157–66.

130. Grote JP, Zeradjanin AR, Cherevko S, Savan A, Breitbach B, Ludwig A, Mayrhofer KJ. Screening of material libraries for electrochemical CO_2 reduction catalysts—improving selectivity of Cu by mixing with Co. J Catal. 2016;343:248–56.
131. Jedidi A, Rasul S, Masih D, Cavallo L, Takanabe K. Generation of Cu–In alloy surfaces from $CuInO_2$ as selective catalytic sites for CO_2 electroreduction. J Mater Chem A. 2015;3(37):19085–92.
132. Rasul S, Anjum DH, Jedidi A, Minenkov Y, Cavallo L, Takanabe K. A highly selective copper–indium bimetallic electrocatalyst for the electrochemical reduction of aqueous CO_2 to CO. Angew Chem Int Ed. 2015;54(7):2146–50.
133. Li D, Wu J, Liu T, Liu J, Yan Z, Zhen L, Feng Y. Tuning the pore structure of porous tin foam electrodes for enhanced electrochemical reduction of carbon dioxide to formate. Chem Eng J. 2019;375:122024.
134. Sarfraz S, Garcia-Esparza AT, Jedidi A, Cavallo L, Takanabe K. Cu–Sn bimetallic catalyst for selective aqueous electroreduction of CO_2 to CO. ACS Catal. 2016;6(5):2842–51.
135. Cheng J, Xuan X, Yang X, Zhou J, Cen K. Selective reduction of CO_2 to alcohol products on octahedral catalyst of carbonized Cu(BTC) doped with Pd nanoparticles in a photoelectrochemical cell. Chem Eng J. 2019;358:860–8.
136. Hsieh YC, Senanayake SD, Zhang Y, Xu W, Polyansky DE. Effect of chloride anions on the synthesis and enhanced catalytic activity of silver nanocoral electrodes for CO_2 electroreduction. ACS Catal. 2015;5(9):5349–56.
137. Furuya N, Yamazaki T, Shibata M. High performance Ru–Pd catalysts for CO_2 reduction at gas-diffusion electrodes. J Electroanal Chem. 1997;431(1):39–41.
138. Back S, Yeom MS, Jung Y. Active sites of Au and Ag nanoparticle catalysts for CO_2 electroreduction to CO. ACS Catal. 2015;5(9):5089–96.
139. Dunfeng Gao H, Zhou JW, Miao S, Yang F, Wang G, Wang J, Bao X. Size-dependent electrocatalytic reduction of CO_2 over Pd nanoparticles. J Am Chem Soc. 2015;137(13):4288–91.
140. Reske R, Mistry H, Behafarid F, Roldan Cuenya B, Strasser P. Particle size effects in the catalytic electroreduction of CO_2 on Cu nanoparticles. J Am Chem Soc. 2014;136(19):6978–86.
141. Mistry H, Reske R, Zeng Z, Zhao ZJ, Greeley J, Strasser P, Cuenya BR. Exceptional size-dependent activity enhancement in the electroreduction of CO_2 over Au nanoparticles. J Am Chem Soc. 2014;136(47):16473–6.
142. Salehi-Khojin A, Jhong HR, Rosen BA, Zhu W, Ma S, Kenis PJ, Masel RI. Nanoparticle silver catalysts that show enhanced activity for carbon dioxide electrolysis. J Phys Chem C. 2013;117(4):1627–32.
143. Zhang S, Kang P, Meyer TJ. Nanostructured tin catalysts for selective electrochemical reduction of carbon dioxide to formate. J Am Chem Soc. 2014;136(5):1734–7.
144. Xie J, Huang Y, Hanqing Yu. Tuning the catalytic selectivity in electrochemical CO_2 reduction on copper oxide-derived nanomaterials. Front Environ Sci Eng. 2015;9(5):861–6.
145. Dutta A, Rahaman M, Luedi NC, Mohos M, Broekmann P. Morphology matters: tuning the product distribution of CO_2 electroreduction on oxide-derived Cu foam catalysts. ACS Catal. 2016;6(6):3804–14.
146. Ma M, Djanashvili K, Smith WA. Selective electrochemical reduction of CO_2 to CO on CuO-derived Cu nanowires. Phys Chem Chem Phys. 2015;17(32):20861–7.
147. Mariano RG, McKelvey K, White HS, Kanan MW. Selective increase in CO_2 electroreduction activity at grain-boundary surface terminations. Science. 2017;358(6367):1187–92.
148. Feng X, Jiang K, Fan S, Kanan MW. Grain-boundary-dependent CO_2 electroreduction activity. J Am Chem Soc. 2015;137(14):4606–9.
149. Mistry H, Choi YW, Bagger A, Scholten F, Bonifacio CS, Sinev I, Divins NJ, Zegkinoglou I, Jeon HS, Kisslinger K, Stach EA, et al. Enhanced carbon dioxide electroreduction to carbon monoxide over defect-rich plasma-activated silver catalysts. Angew Chem Int Ed. 2017;56(38):11394–8.
150. Eilert A, Cavalca F, Roberts FS, Osterwalder J, Liu C, Favaro M, Crumlin EJ, Ogasawara H, Friebel D, Pettersson LG, Nilsson A. Subsurface oxygen in oxide-derived copper electrocatalysts for carbon dioxide reduction. J Phys Chem Lett. 2017;8(1):285–90.
151. Favaro M, Xiao H, Cheng T, Goddard WA, Crumlin EJ. Subsurface oxide plays a critical role in CO_2 activation by Cu(111) surfaces to form chemisorbed CO_2, the first step in reduction of CO_2. Proc Natl Acad Sci USA. 2017;114(26):6706–11.
152. Xiao J, Kuc A, Frauenheim T, Heine T. CO_2 reduction at low overpotential on Cu electrodes in the presence of impurities at the subsurface. J Mater Chem A. 2014;2(14):4885–9.
153. Cavalca F, Ferragut R, Aghion S, Eilert A, Diaz-Morales O, Liu C, Koh AL, Hansen TW, Pettersson LG, Nilsson A. Nature and distribution of stable subsurface oxygen in copper electrodes during electrochemical CO_2 reduction. J Phys Chem C. 2017;121(45):25003–9.
154. Fields M, Hong X, Nørskov JK, Chan K. Role of subsurface oxygen on Cu surfaces for CO_2 electrochemical reduction. J Phys Chem C. 2018;122(28):16209–15.
155. Lum Y, Ager JW. Stability of residual oxides in oxide-derived copper catalysts for electrochemical CO_2 reduction investigated with 18o labeling. Angew Chem Int Ed. 2018;57(2):551–4.
156. Garza AJ, Bell AT, Head-Gordon M. Is subsurface oxygen necessary for the electrochemical reduction of CO_2 on copper? J Phys Chem Lett. 2018;9(3):601–6.
157. Cheng T, Xiao H, Goddard WA. Nature of the active sites for CO reduction on copper nanoparticles; suggestions for optimizing performance. J Am Chem Soc. 2017;139(34):11642–5.
158. Xiao H, Goddard WA, Cheng T, Liu Y. Cu metal embedded in oxidized matrix catalyst to promote CO_2 activation and CO dimerization for electrochemical reduction of CO_2. Proc Natl Acad Sci USA. 2017;114(26):6685–8.
159. Fisica C, Milano U. And applied chemistry commission on electrochemistry * real surface area measurements prepared for publication by. Pure Appl Chem. 1991;63(5):711–34.
160. McCrory CC, Jung S, Peters JC, Jaramillo TF. Benchmarking heterogeneous electrocatalysts for the oxygen evolution reaction. J Am Chem Soc. 2013;135(45):16977–87.
161. Rendón-Calle A, Builes S, Calle-Vallejo F. A brief review of the computational modeling of CO_2 electroreduction on Cu electrodes. Curr Opin Electrochem. 2018;9:158–65.
162. Nørskov JK, Rossmeisl J, Logadottir A, Lindqvist L, Kitchin JR, Bligaard T, Jónsson H. Origin of the overpotential for oxygen reduction at a fuel-cell cathode. J Phys Chem B. 2004;108(46):17886–92.

163. Chen R, Chen D, Xiao Y. Theoretical scanning of bimetallic alloy for designing efficient N2 electroreduction catalyst. Mater Today Energy. 2021;20:100684.
164. Xiao Y, Tang L, Zhang W, Shen C. Theoretical insights into the selective and activity of CuAu catalyst for O2 and CO_2 electroreduction. Comput Mater Sci. 2021;192:110402.
165. Sakong S, Naderian M, Mathew K, Hennig RG, Grob A. Density functional theory study of the electrochemical interface between a Pt electrode and an aqueous electrolyte using an implicit solvent method. J Chem Phys. 2015;142(23):234107.
166. Rasmussen PB, Holmblad PM, Askgaard T, Ovesen CV, Stoltze P, Nørskov JK, Chorkendorff I. Methanol synthesis on Cu(100) from a binary gas mixture of CO_2 and H2. Catal Lett. 1994;26(3):373–81.
167. Durand WJ, Peterson AA, Studt F, Abild-Pedersen F, Nørskov JK. Structure effects on the energetics of the electrochemical reduction of CO_2 by copper surfaces. Surf Sci. 2011;605(15):1354–9.
168. Calle-Vallejo F, Loffreda D, Koper M, Sautet P. Introducing structural sensitivity into adsorption-energy scaling relations by means of coordination numbers. Nat Chem. 2015;7(5):403–10.
169. Tymoczko J, Calle-Vallejo F, Schuhmann W, Bandarenka AS. Making the hydrogen evolution reaction in polymer electrolyte membrane electrolysers even faster. Nat Commun. 2016;7(1):10990.
170. Calle-Vallejo F, Martínez JI, García-Lastra JM, Sautet P, Loffreda D. Fast prediction of adsorption properties for platinum nanocatalysts with generalized coordination numbers. Angew Chem Int Ed. 2014;53(32):8316–9.
171. Tang W, Peterson AA, Varela AS, Jovanov ZP, Bech L, Durand WJ, Dahl S, Nørskov JK, Chorkendorff I. The importance of surface morphology in controlling the selectivity of polycrystalline copper for CO_2 electroreduction. Phys Chem Chem Phys. 2012;14(1):76–81.
172. Hirunsit P. Electroreduction of carbon dioxide to methane on copper, copper–silver, and copper–gold catalysts: a DFT study. J Phys Chem C. 2013;117(16):8262–8.
173. Hirunsit P, Soodsawang W, Limtrakul J. CO_2 electrochemical reduction to methane and methanol on copper-based alloys: theoretical insight. J Phys Chem C. 2015;119(15):8238–49.
174. Hansen HA, Shi C, Lausche AC, Peterson AA, Nørskov JK. Bifunctional alloys for the electroreduction of CO_2 and CO. Phys Chem Chem Phys. 2016;18(13):9194–201.
175. Jovanov ZP, Hansen HA, Varela AS, Malacrida P, Peterson AA, Nørskov JK, Stephens IE, Chorkendorff I. Opportunities and challenges in the electrocatalysis of CO_2 and CO reduction using bifunctional surfaces: a theoretical and experimental study of Au–Cd alloys. J Catal. 2016;343:215–31.
176. Calle-Vallejo F, Koper MT. Accounting for bifurcating pathways in the screening for CO_2 reduction catalysts. ACS Catal. 2017;7(10):7346–51.
177. Nie X, Luo W, Janik MJ, Asthagiri A. Reaction mechanisms of CO_2 electrochemical reduction on Cu(111) determined with density functional theory. J Catal. 2014;312:108–22.
178. Hussain J, Skúlason E, Jónsson H. Computational study of electrochemical CO_2 reduction at transition metal electrodes. Procedia Comput Sci. 2015;51:1865–71.
179. Luo J, Fan RQ, Wang T, Gao Y, Liu LZ, Yan SH, Zhang ZH. Evaluation of spent pig litter compost as a peat substitute in soilless growth media. Biol Agric Hortic. 2015;31(4):219–29.
180. Ledezma-Yanez I, Gallent EP, Koper MT, Calle-Vallejo F. Structure-sensitive electroreduction of acetaldehyde to ethanol on copper and its mechanistic implications for CO and CO_2 reduction. Catal Today. 2016;262:90–4.
181. Montoya JH, Peterson AA, Nørskov JK. Insights into cc coupling in CO_2 electroreduction on copper electrodes. ChemCatChem. 2013;5(3):737–42.
182. Rahaman M, Dutta A, Zanetti A, Broekmann P. Electrochemical reduction of CO_2 into multicarbon alcohols on activated Cu mesh catalysts: an identical location (IL) study. ACS Catal. 2017;7(11):7946–56.
183. Ting LR, García-Muelas R, Martín AJ, Veenstra FL, Chen ST, Peng Y, Per EY, Pablo-García S, López N, Pérez-Ramírez J, Yeo BS. Electrochemical reduction of carbon dioxide to 1-butanol on oxide-derived copper. Angew Chem. 2020;132(47):21258–65.
184. Hori Y, Murata A, Takahashi R, Suzuki S. Enhanced formation of ethylene and alcohols at ambient temperature and pressure in electrochemical reduction of carbon dioxide at a copper electrode. J Chem Soc Chem Commun. 1988;1:17–9.
185. Frese KW. Electrochemical reduction of CO2 at intentionally oxidized copper electrodes. J Electrochem Soc. 1991;138(11):3338.
186. Ebaid M, Jiang K, Zhang Z, Drisdell WS, Bell AT, Cooper JK. Production of C2/C3 oxygenates from planar copper nitride-derived mesoporous copper via electrochemical reduction of CO_2. Chem Mater. 2020;32(7):3304–11.
187. Hori Y, Takahashi I, Koga O, Hoshi N. Selective formation of C2 compounds from electrochemical reduction of CO_2 at a series of copper single crystal electrodes. J Phys Chem B. 2002;106(1):15–7.
188. Kas R, Kortlever R, Milbrat A, Koper MTM, Mul G, Baltrusaitis J. Electrochemical CO_2 reduction on Cu_2O-derived copper nanoparticles: controlling the catalytic selectivity of hydrocarbons. Phys Chem Chem Phys. 2014;16(24):12194–201.
189. Mi Y, Shen S, Peng X, Bao H, Liu X, Luo J. Selective electroreduction of CO_2 to C2 products over Cu_3N-derived Cu nanowires. ChemElectroChem. 2019;6(9):2393–7.
190. Veenstra FLP, Martín AJ, Pérez-Ramírez J. Nitride-derived copper modified with indium as a selective and highly stable catalyst for the electroreduction of carbon dioxide. Chemsuschem. 2019;12(15):3501.
191. Liang ZQ, Zhuang TT, Seifitokaldani A, Li J, Huang CW, Tan CS, Li Y, De Luna P, Dinh CT, Hu Y, et al. Copper-on-nitride enhances the stable electrosynthesis of multi-carbon products from co 2. Nat Commun. 2018;9(1):1–8.
192. Yin Z, Chao Yu, Zhao Z, Guo X, Shen M, Li N, Muzzio M, Junrui Li H, Liu HL, et al. Cu_3N nanocubes for selective electrochemical reduction of CO_2 to ethylene. Nano Lett. 2019;19(12):8658–63.
193. Alfonso DR, Tafen DN, Kauffmann DR. First-principles modeling in heterogeneous electrocatalysis. Catalysts. 2018;8(10):424.
194. Peterson AA, Abild-Pedersen F, Studt F, Rossmeisl J, Nørskov JK. How copper catalyzes the electroreduction of carbon dioxide into hydrocarbon fuels. Energy Environ Sci. 2010;3(9):1311–5.
195. Russell AE. Electrocatalysis: theory and experiment at the interface. Phys Chem Chem Phys. 2008;10(25):3607–8.
196. Saravanan K, Basdogan Y, Dean J, Keith JA. Computational investigation of CO_2 electroreduction on tin oxide and predictions of Ti, V, Nb and Zr dopants for improved catalysis. J Mater Chem A. 2017;5(23):11756–63.

197. Saravanan K, Gottlieb E, Keith JA. Nitrogen-doped nanocarbon materials under electroreduction operating conditions and implications for electrocatalysis of CO_2. Carbon. 2017;111:859–66.
198. Koper MTM. Theory of multiple proton–electron transfer reactions and its implications for electrocatalysis. Chem Sci. 2013;4(7):2710–23.
199. Koper MTM. Activity volcanoes for the electrocatalysis of homolytic and heterolytic hydrogen evolution. J Solid State Electrochem. 2016;20(4):895–9.
200. Abild-Pedersen F, Greeley J, Studt F, Rossmeisl J, Munter TR, Moses PG, Skúlason E, Bligaard T, Nørskov JK. Scaling properties of adsorption energies for hydrogen-containing molecules on transition-metal surfaces. Phys Rev Lett. 2007;99(1):016105.
201. Montemore MM, Will Medlin J. Scaling relations between adsorption energies for computational screening and design of catalysts. Catal Sci Technol. 2014;4(11):3748–61.
202. Greeley J. Theoretical heterogeneous catalysis: scaling relationships and computational catalyst design. Annu Rev Chem Biomol Eng. 2016;7(1):605–35.
203. Govindarajan N, García-Lastra JM, Meijer EJ, Calle-Vallejo F. Does the breaking of adsorption-energy scaling relations guarantee enhanced electrocatalysis? Curr Opin Electrochem. 2018;8:110–7.
204. Calle-Vallejo F, Krabbe A, García-Lastra JM. How covalence breaks adsorption-energy scaling relations and solvation restores them. Chem Sci. 2016;8(1):124–30.
205. Shin H, Ha Y, Kim H. 2D covalent metals: a new materials domain of electrochemical CO_2 conversion with broken scaling relationship. J Phys Chem Lett. 2016;7(20):4124–9.
206. Li Y, Sun Q. Recent advances in breaking scaling relations for effective electrochemical conversion of CO_2. Adv Energy Mater. 2016;6(17):1–19.
207. Khorshidi A, Violet J, Hashemi J, Peterson AA. How strain can break the scaling relations of catalysis. Nat Catal. 2018;1(4):263–8.
208. Cheng MJ, Kwon Y, Head-Gordon M, Bell AT. Tailoring metal-porphyrin-like active sites on graphene to improve the efficiency and selectivity of electrochemical CO_2 reduction. J Phys Chem C. 2015;119(37):21345–52.
209. Hori Y, Kikuchi K, Suzuki S. Production of co and CH4 in electrochemical reduction of CO_2 at metal electrodes in aqueous hydrogencarbonate solution. Chem Lett. 1985;14(11):1695–8.
210. Kuhl KP, Hatsukade T, Cave ER, Abram DN, Kibsgaard J, Jaramillo TF. Electrocatalytic conversion of carbon dioxide to methane and methanol on transition metal surfaces. J Am Chem Soc. 2014;136(40):14107–13.
211. Schouten KJ, Gallent EP, Koper MT. The influence of pH on the reduction of CO and CO_2 to hydrocarbons on copper electrodes. J Electroanal Chem. 2014;716:53–7.
212. Murata A, Hori Y. Product selectivity affected by cationic species in electrochemical reduction of CO_2 and CO at a Cu electrode. Bull Chem Soc Jpn. 1991;64(1):123–7.
213. Singh MR, Kwon Y, Lum Y, Ager JW III, Bell AT. Hydrolysis of electrolyte cations enhances the electrochemical reduction of CO_2 over Ag and Cu. J Am Chem Soc. 2016;138(39):13006–12.
214. Chen LD, Urushihara M, Chan K, Nørskov JK. Electric field effects in electrochemical CO_2 reduction. ACS Catal. 2016;6(10):7133–9.
215. Resasco J, Chen LD, Clark E, Tsai C, Hahn C, Jaramillo TF, Chan K, Bell AT. Promoter effects of alkali metal cations on the electrochemical reduction of carbon dioxide. J Am Chem Soc. 2017;139(32):11277–87.
216. Akhade SA, McCrum IT, Janik MJ. The impact of specifically adsorbed ions on the copper-catalyzed electroreduction of CO_2. J Electrochem Soc. 2016;163(6):F477–84.
217. Varela AS, Wen J, Reier T, Strasser P. Tuning the catalytic activity and selectivity of Cu for CO_2 electroreduction in the presence of halides. ACS Catal. 2016;6(4):2136–44.
218. Ghiringhelli LM, Vybiral J, Levchenko SV, Draxl C, Scheffler M. Big data of materials science: critical role of the descriptor. Phys Rev Lett. 2015;114(10):1–5.
219. Peterson AA, Christensen R, Khorshidi A. Addressing uncertainty in atomistic machine learning. Phys Chem Chem Phys. 2017;19(18):10978–85.
220. Ulissi ZW, Tang MT, Xiao J, Liu X, Torelli DA, Karamad M, Cummins K, Hahn C, Lewis NS, Jaramillo TF, Chan K, Nørskov JK. Machine-learning methods enable exhaustive searches for active bimetallic facets and reveal active site motifs for CO_2 reduction. ACS Catal. 2017;7(10):6600–8.
221. Liu SP, Zhao M, Gao W, Jiang Q. Mechanistic insights into the unique role of copper in CO_2 electroreduction reactions. ChemSusChem. 2017;10(2):387–93.
222. Ma X, Li Z, Achenie LE, Xin H. Machine-learning-augmented chemisorption model for CO_2 electroreduction catalyst screening. J Phys Chem Lett. 2015;6(18):3528–33.
223. Zhong M, Tran K, Min Y, Wang C, Wang Z, Dinh C-T, De Luna P, Zongqian Yu, Rasouli AS, Brodersen P, Sun S, Voznyy O, Tan C-S, Askerka M, Che F, Liu M, Seifitokaldani A, Pang Y, Lo S-C, Ip A, Ulissi Z, Sargent EH. Accelerated discovery of CO_2 electrocatalysts using active machine learning. Nature. 2020;581(7807):178–83.